Track-to-Track Fusion Using Inside Information From Local IMM Estimators

RADU VISINA
YAAKOV BAR-SHALOM
PETER WILLETT
DIPAK K. DEY

A novel approach to the track-to-track fusion (T2TF) of state estimates from interacting multiple-model (IMM) estimators using inside information [mode-conditioned estimates (MCEs) and mode probabilities] is described in this paper. Fusion is performed on-demand, i.e., without conditioning on past track data. The local trackers run IMM estimators to track a maneuvering target with switching process noise and they transmit MCEs and mode probabilities to a fusion center. The fused state posterior probability density is a Gaussian mixture, where the parameters of the required likelihood functions can be computed recursively. Mode probabilities are fused by transforming them to log-ratios and using them as statistical information in the likelihood function of the mode. This results in consistent data fusion based on known target and local tracker (IMM) parameters. Simulations show that this method outperforms the fusion of the local IMM estimator Gaussian-approximated outputs both in terms of error during target maneuvers and in terms of the consistency of the mean-squared error (MSE). It is a generalization of Gaussian T2TF with crosscovariance, and its performance is close to that of centralized measurement fusion (CMF)—by accounting for the error and log-ratio crosscovariances, the fused covariance consistency matches the ideal consistency of CMF without requiring memory of past fused tracks. The method is also shown to be more accurate, informative, consistent in MSE, and of lower computational and communication cost than Chernoff fusion, a recently published method for Gaussian mixture fusion.

Manuscript received May 7, 2019; revised December 11, 2019 and June 10, 2020; released for publication July 27, 2020.

This work was supported in part by NSWC under Grant N001741810004.

Refereeing of this contribution was handled by Chee-Yee Chong.

The authors are with the University of Connecticut, Storrs, CT 06269-4157 USA (E-mail: radu.visina, yaakov.bar-shalom, peter.willett, dipak.dey@uconn.edu).

1557-6418/20/$17.00

I. INTRODUCTION

The interacting multiple model (IMM) estimator is a powerful nonlinear state estimator for targets whose dynamic evolution model changes according to a discrete-time, discrete-state Markov chain with known transition probabilities, and it may be used in local estimators for tracking maneuvering targets or other mode-switching systems. In this work, the posterior probability density function (PDF) of the state of a dynamic target, conditioned on information from local trackers (LTs) implementing the IMM estimation algorithm [4], is derived for on-demand track-to-track fusion (T2TF). The LTs provide Gaussian mixture track information from inside their IMM algorithms [the current mode-conditioned estimates (MCEs) and mode probabilities]. The fusion center (FC) continuously updates a linearized system description of the IMM estimator's error and mode probability behavior to compute the required parameters of the likelihood functions of the state and mode. The fused posterior state PDF is then approximated as a Gaussian mixture.

When new measurements from every sensor can be communicated to a FC at every measurement time, the optimal solution is to stack all new measurements into a single vector and run a single estimator, resulting in optimal centralized measurement fusion (CMF) [5]. However, data may need to be sent at arbitrarily low rates compared to the LT measurement intervals, requiring the transmission of recursively computed local estimates (and sometimes covariances). The problem is difficult because of the dependent nature of the received state estimation errors. The correlation between the local estimation errors was described in [2] and [3] as the recursively-computed crosscovariance matrices for linear, Gaussian estimators, and their incorporation into the standard fusion equations results in optimal fusion (given only the on-demand tracks) and consistent fused covariances. This method is termed Gaussian T2TF with crosscovariance (GT2TFwXC) and requires knowledge of the Kalman filter design parameters.

The recursive computations described in this paper yield the required matrices (including crosstracker and crossmode covariances) for IMM track fusion as a multiple-model generalization of GT2TFwXC. For a single mode, the algorithm reduces naturally to GT2TFwXC. Just as GT2TFwXC requires knowledge of the LT Kalman filter parameters and the target, this paper's proposed method also requires the parameters of the LT IMM estimators and the target. To bound the complexity of the problem, the proposed method is derived for trackers that agree on the set of possible dynamic target maneuvering modes and the mode transition probabilities. The information from the trackers is for the same times (i.e., it is synchronous). It is also assumed that the target state transition matrix is the same in both modes, so the method is ideal for target models that switch process noise covariance only.

(Section III-E explains the difficulty encountered with a switching transition matrix.) The assumptions stated here serve to introduce important theory from which additional complexities can be included in future work. The proposed method, along with the theory supporting it, are the foundations for on-demand T2TF from multiple-model trackers.

For the fusion of IMM mode-conditioned information, the extraction of track information from mode probabilities (i.e., the mixture weights) is an additional problem. This suggests that the received probabilities should be treated as statistical information in the conditioning of the posterior (fused) PDF. To account for the dependency between the received probabilities, they are transformed into infinite-support *log-ratios (LRs) of probabilities* and a linear approximation of their evolution is derived. Using this technique, the local mode probabilities are successfully combined to form the fused mode probabilities with the same number of modes, allowing for mode inference based on the fused information.

As an alternative, T2TF can be performed naively using the LT's moment-matched IMM output estimate and covariance [11], but that method has poor performance during maneuvers and does not account for error cross-covariance.

An alternate Gaussian mixture fusion approach has been explored—Chernoff fusion, first proposed by Mahler [13] and Hurley [10], has received some attention in the literature, and is capable of minimizing the fused mean-squared error (MSE) while assuring that the fused covariance is greater than or equal to the actual sample MSE, without direct knowledge of the error crosscovariances. A successful, computationally feasible implementation for Gaussian mixtures using unscented sigma points has been developed in [8] and used in distributed fusion from IMM tracks in [9]. However, Chernoff fusion is unable to exploit system model information (i.e., target dynamic motion models and IMM design parameters, assumed available in this paper) and may produce fused covariance values that are too high, though they acceptably represent the sample MSE of the fused estimate (i.e., the covariances are consistent). The sigma point implementation is still computationally demanding due to the need to search for the optimal fusion exponent, and requires the transmission of local mode-conditioned estimate covariances. Just as the IMM fusion proposed here generalizes GT2TFwXC, Chernoff fusion generalizes the covariance intersection method and solves the fusion problem when the crosscovariance cannot be computed or because system parameters (local IMM parameters) are not available. While ignoring crosscovariances altogether results in overly optimistic fused covariances, Chernoff Fusion results in conservative fused covariances, which are still not ideal, meaning that the MSE is higher than what is possible with a more optimal method. When the target and LT system design parameters are known, the crosscovariances can be computed recursively and Bayesian fusion can be performed as shown in this paper without the transmission of the local covariance matrices and without the need for numerical optimization. The simulation results show that although the fused covariance of the Chernoff method match the MSE of the fused estimate, the model-driven fusion with crosscovariance presented here significantly outperforms Chernoff fusion in terms of fused accuracy. Another advantage of the method in this paper is that the fused probability density output includes fused mixture probabilities, which directly provide inference about target dynamic maneuvering mode. Chernoff fusion cannot provide this output information because the number of mixture components in its fused PDF is a product of the number of local components, and such a mixture has no event-based interpretation in the multiple-model target maneuvering scenario.

Another approach to the fusion of Gaussian mixture filter outputs was developed in [14]. That paper introduces the topic of crosscovariances for every mixture component. However, that approach mainly treats problems with Gaussian mixture process noise and Gaussian mixture measurement PDFs, both of which are unlike the Markov chain switching processes involved in maneuvering target tracking. Additionally, there is no consideration of mixture component reduction strategies that complicate the crosscovariance structure (such as the mixing process of the IMM estimator); they assume fully invertible state-to-measurement equations (unrealistic in target tracking applications where the state vector is longer than the measurement vector), and do not consider the dependent, stochastic nature of local mixture probabilities (weights) in their fused mixture probabilities. The method developed in this paper accounts for the Markov chain process of the target maneuvers and the mixing process of the IMM, does not require invertible measurement equations, and fully computes the crosscovariances between all local mode-conditioned state estimates and mode probabilities at the FC.

Though the present method does not require memory of past fused tracks, alternative data fusion schemes exist that utilize memory of past fused tracks and decorrelate the information being passed throughout a distributed sensing network. One of the first such algorithms for Gaussian tracks was Information Matrix Fusion [5]. See [6] and [7] for a general discussion of recent advancements in distributed tracking. An approximate method to solve this for IMM tracks was developed in [12]. A model-agnostic method for fusion of IMM Gaussian mixture tracks with memory was also developed in [1]. These methods do not provide the crosscovariance for fusion without past track information. Given these distinctions, further comparison is outside of the scope of this paper; however, it should be noted that, theoretically fusion schemes with memory running at full rate could yield the accuracy performance of CMF (which is slightly more accurate than on-demand fusion techniques [5]), but the results in this paper show

that the present memoryless method still achieves fused track accuracy close to that of CMF and with ideal MSE consistency.

Even when using a suitable reduced-rate T2TF method, the problem of initial fusion must still be solved using an on-demand fusion scheme. Without it, the FC has no initial condition (i.e., prior) for recursive updating of the fused track. This resembles the problem of running a Kalman Filter without a previous estimate and covariance [4], [5]. GT2TFwXC provides a consistent fused estimate without initial conditions for linear Gaussian systems; likewise, this paper shows how this is accomplished when the received tracks come from IMM estimators tracking a maneuvering target.

This paper is organized as follows: Section II introduces the problem mathematically, Section III describes the required Bayesian fusion theory, Section IV develops the algorithmic steps required to implement fusion with IMM inside information, Section V summarizes the algorithm and discusses computational complexity, and Section VI presents Monte Carlo simulations and results. A list of symbols and acronyms is provided in Table 1 for reference.

II. DESCRIPTION OF TARGET AND LOCAL TRACKERS

For clarity, only two LTs and two dynamic modes will be considered, but the extension to multiple trackers and modes is possible. Local state estimation is performed by two trackers obtaining noisy observations of a target whose dynamics may switch between two different modes. Each tracker, indexed $j = 1, 2$, computes MCEs and mode-conditioned covariances (MCCs) of $\mathbf{x}(k)$ from modes indexed $m = 1, 2$. With $\mathbf{Z}_j^k$ as the vector of all measurements at tracker j, up to and including the present time step,

$$\mathbf{Z}_j^k = \left[\mathbf{z}_j(0)'\ \mathbf{z}_j(1)'\ \ldots\ \mathbf{z}_j(k)'\right]', \tag{1}$$

the N_x-dimensional MCEs, conditioned on the current target mode $M(k)$ being m, are denoted and defined as

$$\hat{\mathbf{x}}_j^m(k|k) \triangleq E[\mathbf{x}(k) \mid \mathbf{Z}_j^k, M(k) = m], \quad \begin{matrix} j = 1, 2, \\ m = 1, 2 \end{matrix} \tag{2}$$

and with the MCE errors (MCEEs) defined as

$$\tilde{\mathbf{x}}_j^m(k|k) = \hat{\mathbf{x}}_j^m(k|k) - \mathbf{x}(k), \tag{3}$$

the MCCs are

$$\mathbf{P}_j^m(k|k) \triangleq E\left[\tilde{\mathbf{x}}_j^m(k|k)\tilde{\mathbf{x}}_j^m(k|k)' \mid \mathbf{Z}_j^k, M(k) = m\right]. \tag{4}$$

The true state of the target, when in mode $M(k) = n$, evolves linearly in time as[1]

$$\mathbf{x}^{|n}(k+1) = \mathbf{F}\mathbf{x}(k) + \mathbf{v}^n(k). \tag{5}$$

The N_z-dimensional measurements of the target at each tracker are obtained according to

$$\mathbf{z}_j(k) = \mathbf{H}_j\mathbf{x}(k) + \mathbf{w}_j(k). \tag{6}$$

The trackers compute the probability of the target being in mode m at time step k as

$$\mu_j^m(k) \triangleq \mathrm{P}\left(M(k) = m \mid \mathbf{Z}_j^k\right). \tag{7}$$

The evolution of the target's dynamic modes is modeled as a Markov chain. Its known transition probability matrix (TPM; [4]) is

$$\Pi = \begin{bmatrix} \pi^{11} & \pi^{12} \\ \pi^{21} & \pi^{22} \end{bmatrix} \tag{8}$$

and all of its rows must have a sum of 1.

Two key simplifying assumptions are made. First, as can be seen in equation (5), mode changes affect the process noise only and not the state transition matrix $\mathbf{F}$. This simplification was made because the theory required to fuse with switching $\mathbf{F}$ becomes much more involved, especially if the state space of the models switches dimension. It is important to note that the methods developed in this paper are the foundations of a unique methodology in on-demand T2TF that can be extended to more complexities in future work (see Section III-E). The Bayesian derivation of Gaussian mixture posteriors, along with obtaining the parameters of the likelihood function(s) through *linearization and recursion* of the joint system describing the trackers and the target, constitutes the powerful, yet fundamental, stochastic systems approach to T2TF proposed in this paper.

The second simplification in this paper is that mode switching does not affect the measurement equation (6). Mode-specific measurement parameters can be substituted if required, as long as they switch as part of the same Markov chain process of the target. Given the independence of the target motion and measurement system(s), such examples are not typical in tracking scenarios, so treatment of this case is beyond the scope of this paper.

III. BAYESIAN THEORY FOR IMM INSIDE INFORMATION FUSION

A. The Posterior Fused State PDF

Omitting the time-step index k for brevity, the posterior state PDF of the target state using the data from

[1]Note that m is the index of the MCE at the LT. The FC must consider the received MCE and probabilities under all mode hypotheses, so n is used in the multiple-model inference process at the FC, while m is used only to index the received data.

Table 1
List of Symbols and Acronyms

$\bar{(\cdot)}$	Mean of $(\cdot)$
$\breve{(\cdot)}$	Mixed initial condition of $(\cdot)$ (IMM algorithm)
$\hat{(\cdot)}$	Estimate of $(\cdot)$
$\tilde{(\cdot)}$	Error of $\hat{(\cdot)}$
$\mathbf{d}_j^{\vert n}(k)$	Gaussian-approximated process noise entering the LR
$\mathbf{D}_j^{\vert n}(k)$	Covariance of $\mathbf{d}_j(k)$
$\mathbf{F}$	State transition matrix
$\mathbf{g}^{\vert n}(k)$	Additive noise of the linearized joint IMM system
$\mathbf{G}^{\vert n}(k)$	Covariance of $\mathbf{g}(k)$
$\mathbf{H}_j$	Measurement matrix at LT j
$\mathbf{I}_{N\times N}$	$N \times N$ identity matrix
j	LT index ($j = 1, 2$ — used as a subscript)
$\mathbf{J}^{\vert n}(k)$	Transition Jacobian matrix of the joint IMM system
k	Discrete time step
LR	Log-ratio(s) of probability pair(s)
LT	Local tracker(s)
m	Target mode index of the received estimates and probabilities ($m = 1, 2$ — used as a superscript)
MCC	Local mode-conditioned estimate covariance
MCE(E)	Local mode-conditioned estimate (error)
MCI	Local mode-conditioned innovation (i.e. residual)
MCP(E)	Local mode-conditioned prediction (error)
$M(k)$	True target dynamic mode
$\mu_j^m(k)$	Locally-computed probability of mode m
$\mu_j(k)$	$[\mu_j^1(k) \quad \mu_j^2(k)]'$
$\mu_j^{lm}(k)$	Initial condition mixing weight (IMM algorithm)
n	Target mode index hypothesis under consideration at the FC ($n = 1, 2$)
$(\cdot)^{\vert n}$	Any variable $(\cdot)$ derived under the hypothesis that the current mode is n
$\nu_j^m(k)$	MCI
$\mathbf{N}_j^{lm}$	Spread-of-the-means term of a mixture's covariance
$\omega_j(k)$	LR of the mode based on $\mu_j^1(k\vert k)$
$\mathbf{\Omega}_j^{\vert n}(k)$	Covariance of $[\omega_1(k)\ \omega_2(k)]'$
$p(\cdot)$	Any probability density function (PDF)
$P(\cdot)$	Any probability mass function (PMF)
$\mathbf{P}_{\mathrm{F}}(k)$	Covariance of the moment-matched fused estimate output error
$\mathbf{P}_{\mathrm{F}}^n(k)$	Covariance of the fused nth MCEE
$\mathbf{P}_j^m(k\vert k)$	Locally-computed covariance of $\tilde{\mathbf{x}}_j^m(k\vert k)$ (MCC)
$\breve{\mathbf{P}}_j^m(k\vert k)$	Locally-computed covariance of $\breve{\mathbf{x}}_j^m(k\vert k)$
$\mathbf{P}^{\vert n}(k\vert k-1)$	FC-computed complete covariance/crosscovariance of $\tilde{\mathbf{x}}_j^m(k\vert k-1)$
$\mathbf{P}^{\vert n}(k)$	FC-computed complete covariance/crosscovariance of the MCEE
$\phi_j(k)$	Received data from LT j
π^{lm}	Markov Chain transition probability from mode l to mode m
$\mathbf{Q}^n$	Covariance of the process noise under mode n
$\mathbf{R}_j$	Covariance of measurement error at LT j
$\mathbf{S}^{\vert n}(k)$	FC-computed complete covariance/crosscovariance of the MCI
$\mathbf{S}_j^m(k)$	Locally-computed covariances of $\nu_j^m(k)$
TPM	Transition probability matrix of Markov chain
$\mathbf{v}^n(k)$	Zero mean process noise under mode n
$\mathbf{w}_j(k)$	Zero mean measurement error at LT j
$\mathbf{W}_j^m(k)$	Locally computed Kalman gain matrices
$\mathbf{x}_{\mathrm{F}}(k)$	Moment-matched fused estimate output
$\hat{\mathbf{x}}_{\mathrm{F}}^{\vert n}(k)$	Fused nth MCE
$\breve{\mathbf{x}}_j^m(k\vert k)$	mth mode's mixed initial conditions (from IMM algorithm)
$\hat{\mathbf{x}}_j^m(k\vert k-1)$	Local tracker MCP
$\tilde{\mathbf{x}}_j^m(k\vert k-1)$	Local tracker MCPE
$\hat{\mathbf{x}}_j^m(k\vert k)$	Local tracker MCE
$\tilde{\mathbf{x}}_j^m(k\vert k)$	Local tracker MCEE
$\mathbf{x}(k)$	True target state
$\mathbf{y}^{\vert n}(k)$	"State vector" of the joint IMM system, computed at the FC
$\mathbf{Y}^{\vert n}(k)$	Covariance of $\mathbf{y}^{\vert n}(k)$
$\mathbf{z}_j(k)$	Measurement at LT j

two trackers is a mixture density described by

$$p(\mathbf{x} \mid \phi_1, \phi_2) = \sum_{n=1}^{2} p(\mathbf{x} \mid \phi_1, \phi_2, M = n) P(M = n \mid \phi_1, \phi_2) \tag{9}$$

with the received data from the two trackers (MCE and mode probabilities) defined as

$$\phi_j \triangleq \left\{\hat{\mathbf{x}}_j^1(k|k), \hat{\mathbf{x}}_j^2(k|k), \mu_j^1(k)\right\}, \quad j = 1, 2, \tag{10}$$

where $\mu_j^2(k)$ is ignored in equation (10) due to its redundancy.

The FC does not have access to any $\mathbf{z}_j(k)$ or any past $\hat{\mathbf{x}}_j^m(k|k)$, but should provide the best fused estimate and its error covariance when receiving the latest MCE and mode probabilities from all LTs. To do this, the posterior fused mode-conditioned densities $p(\mathbf{x} \mid \phi_1, \phi_2, M = n)$ and posterior fused mode probabilities $P(M = n \mid \phi_1, \phi_2)$ will be derived next.

The LT MCCs $\mathbf{P}_j^m(k|k)$ are not part of the data used for fusion in equation (10) (see Appendix: Property 7), although the authors are not discouraging the transmission of these data if system parameters are unavailable. The fused MSE and covariance consistency from the Monte Carlo simulations of Section VI are extremely close to that of CMF and this offers empirical evidence that the MCCs do not contain significant information about the target state, so considerable communication savings can be achieved if the covariances are not transmitted.

B. The Fused Mode-Conditioned State Estimates

We claim that, conditioned on the received MCE, the received mode probabilities do not contribute additional information about any mode-conditioned state vector. This is proved for the linearized joint system model in Section III-C and Property 3 of the Appendix. So, the fused posterior mode-conditioned PDFs from equation (9) are approximately

$$\begin{aligned} p(\mathbf{x} \mid \phi_1, \phi_2, n) &\approx p\left(\mathbf{x} \mid \hat{\mathbf{x}}_1^1, \hat{\mathbf{x}}_1^2, \hat{\mathbf{x}}_2^1, \hat{\mathbf{x}}_2^2, M = n\right) \\ &= \frac{1}{a} p(\hat{\mathbf{x}}_1^1, \hat{\mathbf{x}}_1^2, \hat{\mathbf{x}}_2^1, \hat{\mathbf{x}}_2^2 \mid M = n, \mathbf{x}) \\ &\quad \times p(\mathbf{x} \mid M = n), \quad n = 1, 2, \end{aligned} \tag{11}$$

with a a normalizing constant and $p(\mathbf{x} \mid M = n)$ considered noninformative (i.e., diffuse) because there is no initial condition about the target state at the FC (the key assumption for on-demand fusion).[2] The likelihood of the state in equation (11) is the PDF of the LT MCE, conditioned on the true state $\mathbf{x}(k)$ and true mode $M(k) = n$, given as

$$p(\hat{\mathbf{x}}_1^1, \hat{\mathbf{x}}_1^2, \hat{\mathbf{x}}_2^1, \hat{\mathbf{x}}_2^2 \mid M = n, \mathbf{x}) \tag{12}$$

with mean

$$E\left\{\left[(\hat{\mathbf{x}}_1^1)' (\hat{\mathbf{x}}_1^2)' (\hat{\mathbf{x}}_2^1)' (\hat{\mathbf{x}}_2^2)'\right]' \mid M = n, \mathbf{x}\right\} = \left[\mathbf{x}' \mathbf{x}' \mathbf{x}' \mathbf{x}'\right]' \tag{13}$$

and covariance (to be computed recursively at the FC as described in Section IV-B)

$$\mathbf{P}^{|n} \triangleq E\left\{\begin{bmatrix} \tilde{\mathbf{x}}_1^1(\tilde{\mathbf{x}}_1^1)' & \tilde{\mathbf{x}}_1^1(\tilde{\mathbf{x}}_1^2)' & \tilde{\mathbf{x}}_1^1(\tilde{\mathbf{x}}_2^1)' & \tilde{\mathbf{x}}_1^1(\tilde{\mathbf{x}}_2^2)' \\ \tilde{\mathbf{x}}_1^2(\tilde{\mathbf{x}}_1^1)' & \tilde{\mathbf{x}}_1^2(\tilde{\mathbf{x}}_1^2)' & \tilde{\mathbf{x}}_1^2(\tilde{\mathbf{x}}_2^1)' & \tilde{\mathbf{x}}_1^2(\tilde{\mathbf{x}}_2^2)' \\ \tilde{\mathbf{x}}_2^1(\tilde{\mathbf{x}}_1^1)' & \tilde{\mathbf{x}}_2^1(\tilde{\mathbf{x}}_1^2)' & \tilde{\mathbf{x}}_2^1(\tilde{\mathbf{x}}_2^1)' & \tilde{\mathbf{x}}_2^1(\tilde{\mathbf{x}}_2^2)' \\ \tilde{\mathbf{x}}_2^2(\tilde{\mathbf{x}}_1^1)' & \tilde{\mathbf{x}}_2^2(\tilde{\mathbf{x}}_1^2)' & \tilde{\mathbf{x}}_2^2(\tilde{\mathbf{x}}_2^1)' & \tilde{\mathbf{x}}_2^2(\tilde{\mathbf{x}}_2^2)' \end{bmatrix} \middle| n, \mathbf{x}\right\}. \tag{14}$$

With equation (14) computed, the solution to equation (11) is the standard linear minimum mean-square error (LMMSE) fusion given by (see [5])

$$\hat{\mathbf{x}}_{\mathrm{F}}^n(k) = \left[\bar{\mathbf{L}}'(\mathbf{P}^{|n})^{-1}\bar{\mathbf{L}}\right]^{-1} \bar{\mathbf{L}}'(\mathbf{P}^{|n})^{-1}\hat{\mathbf{X}} \tag{15}$$

and the corresponding fused covariance given by

$$\mathbf{P}_{\mathrm{F}}^n(k) = \left[\bar{\mathbf{L}}'(\mathbf{P}^{|n})^{-1}\bar{\mathbf{L}}\right]^{-1} \tag{16}$$

with

$$\bar{\mathbf{L}} \triangleq \left[\mathbf{I}_{N_x \times N_x}\ \mathbf{I}_{N_x \times N_x}\ \mathbf{I}_{N_x \times N_x}\ \mathbf{I}_{N_x \times N_x}\right]'. \tag{17}$$

The $4N_x$-element vector $\hat{\mathbf{X}}$ in equation (15) is

$$\hat{\mathbf{X}} = \left[(\hat{\mathbf{x}}_1^1)' (\hat{\mathbf{x}}_1^2)' (\hat{\mathbf{x}}_2^1)' (\hat{\mathbf{x}}_2^2)'\right]'. \tag{18}$$

The LMMSE estimator is equivalent to the Bayes estimator under the Gaussian likelihood assumption with a diffuse prior [5]. Its use is justified because the state variables, position, and velocity are integrated from WNA and the FC has no prior track data, so their prior PDF is diffuse.

C. The LR Transformation of Mode Probabilities

Local mode probabilities are computed at the LT by multivariate Gaussian PDF likelihoods evaluated at the latest local measurements. Therefore, the probabilities

[2] The prior is diffuse because the state vector is composed of position and velocity only, which are integrated states of a white noise acceleration (WNA) driven model (i.e., they are nonstationary processes). Before any data arrive, the priors on these states are diffuse. If a target mode contains states that follow a stationary process, such as Ornstein–Uhlenbeck acceleration, then the acceleration is a stationary process with a proper prior. This may also be true if the **F** matrix is unique for each mode. While fusion can still be performed in a sub-optimal manner by assuming diffuse priors on the target state, the problems of accommodating switching **F** and optimally treating stationary process states will be treated in future work.

are themselves stochastic processes. Since finding a parametric joint PDF of these nonlinear transformations is not feasible, a solution is to transform the probabilities into LRs and use a multivariate Gaussian approximation of the transformed variables. This approximation is appropriate because LRs have infinite support and the multivariate Gaussian density can capture dependencies by nonzero covariances. The means variances and covariances are then readily computed as those of the difference of quadratic forms of Gaussian random variables (the innovations).

The single LR at LT j, denoted as ω_j, is selected to be the log of the ratio of the mode 1 probability to the mode 2 probability as

$$\omega_j = \ln \frac{\mu_j^1}{\mu_j^2}. \tag{19}$$

Note that only a single LR ω_j uniquely determines the probability pair, so the second log-ratio does not need to be included in the analysis of the likelihood function as it certainly does not provide additional information. If there are more than two modes, then any mode probability can serve as the common denominator for all the LRs, but the rest of this paper will concentrate on the two-mode scenario only.

The LR transformation is one-to-one, and the probabilities can be recovered using

$$\mu_j^1 = \frac{e^{\omega_j}}{e^{\omega_j}+1} \quad \mu_j^2 = \frac{1}{e^{\omega_j}+1}. \tag{20}$$

The transformation allows the new variables to be represented as a nonlinear first-order Markov process driven by the wide-sense white MCI $\boldsymbol{\nu}_j^n(k)$ (see Appendix: Property 1) with LT-computed covariances $\mathbf{S}_j^m(k)$. At the LT, the mode probabilities are computed as posterior probabilities using Gaussian likelihood functions [4]:

$$\mu_j^m(k) = \sum_{l=1}^{2} \pi^{lm} \mu_j^l(k-1) \cdot \frac{1}{c} |2\pi \mathbf{S}_j^m(k)|^{-\frac{1}{2}} e^{-\frac{1}{2}\left[\nu_j^m(k)\right]' \left[\mathbf{S}_j^m(k)\right]^{-1} \nu_j^m(k)}. \tag{21}$$

Using equation (21), the normalizing constant c is canceled in the ratio and equation (19) becomes

$$\omega_j(k) = \ln \frac{\pi^{11} e^{\omega_j(k-1)} + \pi^{21}}{\pi^{12} e^{\omega_j(k-1)} + \pi^{22}} + \frac{1}{2} \ln \frac{|\mathbf{S}_j^2(k)|}{|\mathbf{S}_j^1(k)|} + \frac{1}{2} \boldsymbol{\nu}_j^2(k)' \mathbf{S}_j^2(k)^{-1} \boldsymbol{\nu}_j^2(k) - \frac{1}{2} \boldsymbol{\nu}_j^1(k)' \mathbf{S}_j^1(k)^{-1} \boldsymbol{\nu}_j^1(k). \tag{22}$$

The means of the LR processes $\omega_1(k)$, $\omega_2(k)$ are nonzero, and they have a finite variance and nonzero correlation. The first term in equation (22), conditioned on mode n, has the first-order Taylor series expansion around $\breve{\omega}_j^{|n}(k-1)$ (the mixed initial condition—see Section IV-C)

$$\begin{aligned} &\ln \frac{\pi^{11} e^{\omega_j^{|n}(k-1)} + \pi^{21}}{\pi^{12} e^{\omega_j^{|n}(k-1)} + \pi^{22}} \\ &\approx \left[\frac{\pi^{11} e^{\breve{\omega}_j^{|n}(k-1)}}{\pi^{11} e^{\breve{\omega}_j^{|n}(k-1)} + \pi^{21}} - \frac{\pi^{12} e^{\breve{\omega}_j^{|n}(k-1)}}{\pi^{12} e^{\breve{\omega}_j^{|n}(k-1)} + \pi^{22}} \right] \omega_j^{|n}(k-1) \\ &= \left[\breve{\mu}_j^{11|n}(k-1) - \breve{\mu}_j^{12|n}(k-1) \right] \omega_j^{|n}(k-1). \end{aligned} \tag{23}$$

The $\mu_j^{lm|n}$ are the (actual) initial condition mixing weights at the local IMMs, which are functions of the LR, all conditioned on mode n:

$$\begin{aligned} \mu_j^{1m|n}(k-1) &= \frac{\pi^{1m} e^{\omega_j^{|n}(k-1)}}{\pi^{1m} e^{\omega_j^{|n}(k-1)} + \pi^{2m}}, \\ \mu_j^{2m|n}(k-1) &= \frac{\pi^{2m}}{\pi^{1m} e^{\omega_j^{|n}(k-1)} + \pi^{2m}}, \end{aligned} \tag{24}$$

and $\breve{\mu}_j^{lm|n}(k-1)$ are computed according to equation (24) by using $\breve{\omega}_j^{|n}(k-1)$ instead of $\omega_j^{|n}(k-1)$.

The last two terms of equation (22) are the difference of quadratic forms of the innovations, which are correlated between the modes and sensors. Since they are unknown to the FC and they are stochastic, they are considered to be a common additive noise for the LR of both sensors, and the mean and covariance of this noise are readily computed to form a Gaussian approximation.

Omitting k again, the mean and covariance of the LR additive noise can be derived by first defining the stacked vector of the zero mean (see Appendix: Property 1) innovations as

$$\boldsymbol{\nu}^{|n} = \left[(\boldsymbol{\nu}_1^{1|n})' \; (\boldsymbol{\nu}_1^{2|n})' \; (\boldsymbol{\nu}_2^{1|n})' \; (\boldsymbol{\nu}_2^{2|n})' \right]'. \tag{25}$$

The covariance of equation (25) is $\mathbf{S}^{|n}$, derived in Section IV-B. Together with the selection matrices

$$\begin{aligned} \mathbf{L}_1^1 &= [\mathbf{I} \quad \mathbf{0} \quad \mathbf{0} \quad \mathbf{0}] \quad \mathbf{L}_1^2 = [\mathbf{0} \quad \mathbf{I} \quad \mathbf{0} \quad \mathbf{0}] \\ \mathbf{L}_2^1 &= [\mathbf{0} \quad \mathbf{0} \quad \mathbf{I} \quad \mathbf{0}] \quad \mathbf{L}_2^2 = [\mathbf{0} \quad \mathbf{0} \quad \mathbf{0} \quad \mathbf{I}] \end{aligned} \tag{26}$$

the quadratic forms can be written as

$$\begin{aligned} &(\boldsymbol{\nu}_j^{2|n})' (\mathbf{S}_j^2)^{-1} \boldsymbol{\nu}_j^{2|n} - (\boldsymbol{\nu}_j^{1|n})' (\mathbf{S}_j^1)^{-1} \boldsymbol{\nu}_j^{1|n} \\ &= (\boldsymbol{\nu}^{|n})' \left[\left(\mathbf{L}_j^2\right)' (\mathbf{S}_j^2)^{-1} \mathbf{L}_j^2 - \left(\mathbf{L}_j^1\right)' (\mathbf{S}_j^1)^{-1} \mathbf{L}_j^1 \right] \boldsymbol{\nu}^{|n} \\ &= (\boldsymbol{\nu}^{|n})' \mathbf{M}_j \boldsymbol{\nu}^{|n} \triangleq \mathbf{d}^{|n} \end{aligned} \tag{27}$$

with

$$\mathbf{M}_j \triangleq \left(\mathbf{L}_j^2\right)' (\mathbf{S}_j^2)^{-1} \mathbf{L}_j^2 - \left(\mathbf{L}_j^1\right)' (\mathbf{S}_j^1)^{-1} \mathbf{L}_j^1. \tag{28}$$

The hidden matrix $\mathbf{S}_j^m$ is computed at the LT and its expected value can be computed at the FC using the algorithm in Section IV-D and is different from the elements of $\mathbf{S}^{|n}$. The two-dimensional (2D), white,

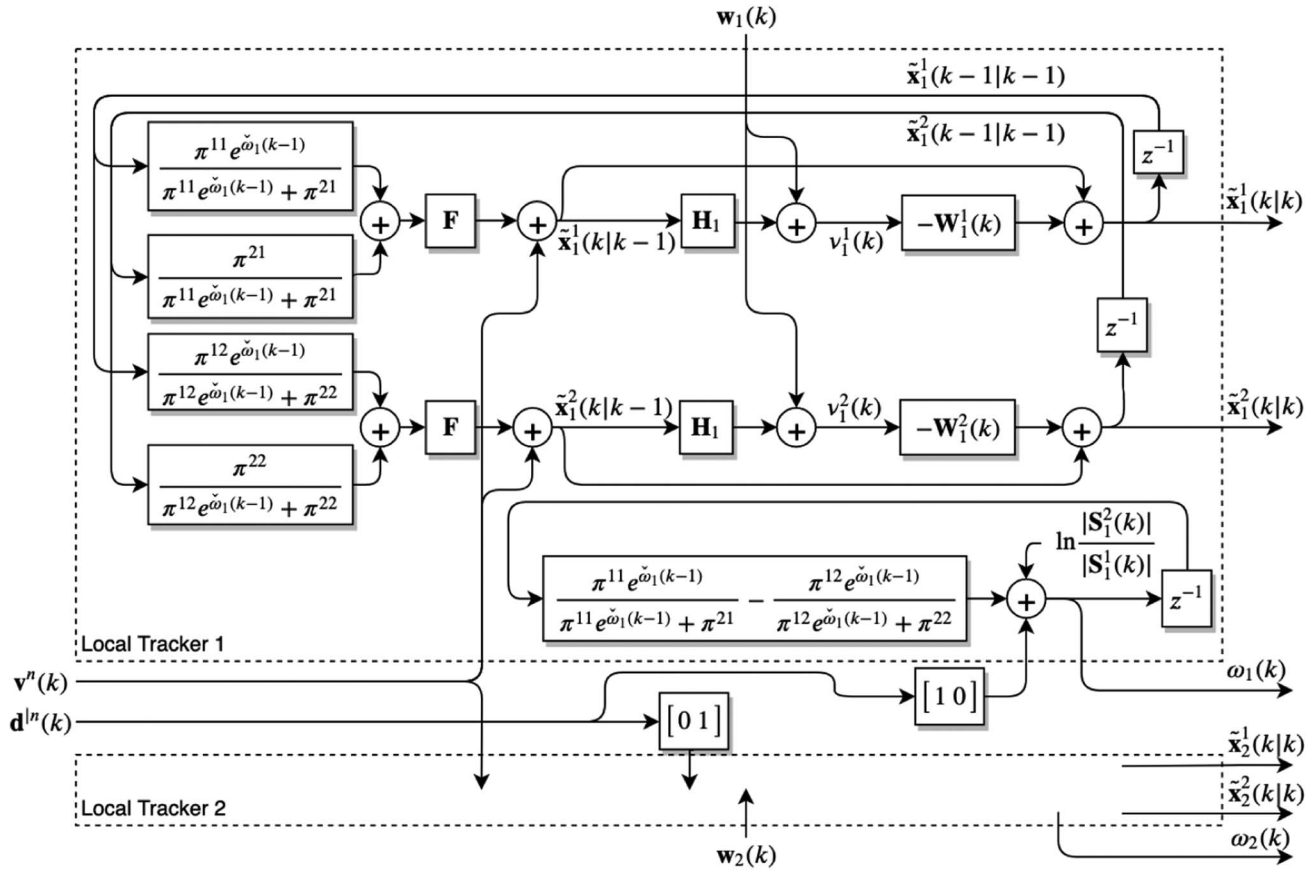

Fig. 1. Block diagram of the linearized model of the mode-conditioned errors and LRs of two IMM LTs (with only one shown explicitly) tracking the same target, from which the computation of the mode-conditioned error covariance, LR mean, and LR covariance can be derived. The evolution of the stochastic matrices $\mathbf{S}_j^m(k)$ and $\mathbf{W}_j^m(k)$ are not shown. Note that this block diagram describes the behavior of the LT but does not describe the fusion algorithm itself. z^{-1} represents a unit delay to indicate variables from the previous time step.

nonzero mean Gaussian random process $\mathbf{d}$ will approximate the quadratic form noise (27), having mean and variance/covariance found by (see [4])

$$\bar{\mathbf{d}}^{|n} \triangleq E[\mathbf{d} \mid n] = \begin{bmatrix} E\left[\boldsymbol{v}'\mathbf{M}_1\boldsymbol{v}\right] \\ E\left[\boldsymbol{v}'\mathbf{M}_2\boldsymbol{v}\right] \end{bmatrix} = \begin{bmatrix} \mathrm{tr}\left[\mathbf{M}_1\mathbf{S}^{|n}\right] \\ \mathrm{tr}\left[\mathbf{M}_2\mathbf{S}^{|n}\right] \end{bmatrix}, \quad (29)$$

$$\mathbf{D}^{|n} \triangleq E\left[(\mathbf{d}-\bar{\mathbf{d}})(\mathbf{d}-\bar{\mathbf{d}})' \mid n\right] = \begin{bmatrix} 2\mathrm{tr}\left[\left(\mathbf{M}_1\mathbf{S}^{|n}\right)^2\right] & 2\mathrm{tr}\left(\mathbf{M}_1\mathbf{S}^{|n}\mathbf{M}_2\mathbf{S}^{|n}\right) \\ 2\mathrm{tr}\left(\mathbf{M}_1\mathbf{S}^{|n}\mathbf{M}_2\mathbf{S}^{|n}\right) & 2\mathrm{tr}\left[\left(\mathbf{M}_2\mathbf{S}^{|n}\right)^2\right] \end{bmatrix}. \quad (30)$$

The covariance between a zero mean Gaussian vector and a quadratic form in the same vector is zero [15]—this means that $\bar{\mathbf{d}}$ is not correlated to the innovations, the process noise, or the measurement noise. See the Appendix for further details regarding this.

D. Fused Mode Probabilities

The received MCEs $\hat{\mathbf{x}}_j^m$ do not contain information about the target mode $M(k)$ (see Appendix: Property 4). Using Bayes' theorem and omitting the time step k for brevity, the posterior fused-mode probabilities are[3]

$$\begin{aligned} \mu_{\mathrm{F}}^n &= P\left(M = n \mid \mu_1^1, \mu_1^2, \mu_2^1, \mu_2^2\right) \\ &= P\left(M = n \mid \omega_1, \omega_2\right) \\ &= \frac{p(\omega_2 \mid \omega_1, M = n)P(M = n \mid \omega_1)}{b} \\ &= \frac{p(\omega_1, \omega_2, \mid M = n)\mu_1^n}{bp(\omega_1 \mid M = n)} \end{aligned} \quad (31)$$

with b the normalizing constant and the likelihood function of the mode based on the LR represented as

$$p(\omega_1, \omega_2 \mid M = n). \quad (32)$$

The goal here is to find the prior mean $[\bar{\omega}_1^{|n}(k)\ \ \bar{\omega}_2^{|n}(k)]'$ and the covariance $\boldsymbol{\Omega}^{|n}(k)$, conditioned under target mode n, of the Gaussian approximation of equation (32) before any data arrive. From this, the marginal in the de-

[3]The representation of equation (31) is not unique—either mode probability can be used as the prior, or the prior can be noninformative. The attractiveness of using a received probability as a prior is the ability to use as much information in the data as possible before the Gaussian approximation. In other words, the ability to directly factor in a probability as a prior can be advantageous from an accuracy perspective.

nominator of equation (31) is easily found and the likelihood can be evaluated for each mode $n = 1, 2$.

E. The LT MCEEs

Recursive covariance computations can be used to find the covariance of the zero mean MCEE. At every step k, there are *two mode hypotheses*, represented by $n = 1, 2$. As in Fig. 1, the error of the mode m prediction at tracker j, conditioned on mode n being the true mode, is

$$\begin{aligned}\tilde{\mathbf{x}}_j^{m|n}(k+1|k) &\triangleq \mathbf{F}\mathbf{x}(k) + \mathbf{v}^n(k) - \mathbf{F}\check{\mathbf{x}}_j^{m|n}(k|k) \\ &= \mathbf{F}\left[\mathbf{x}(k) - \left[\mu_j^{1m|n}\hat{\mathbf{x}}_j^{1|n}(k|k) + \mu_j^{2m|n}\hat{\mathbf{x}}_j^{2|n}(k|k)\right]\right] \\ &\quad + \mathbf{v}^n(k) \\ &= \mathbf{F}\left[\mu_j^{1m|n}\tilde{\mathbf{x}}_j^{1|n}(k|k) + \mu_j^{2m|n}\tilde{\mathbf{x}}_j^{2|n}(k|k)\right] \\ &\quad + \mathbf{v}^n(k).\end{aligned} \tag{33}$$

The MCEEs are propagated from the previous mode-conditioned prediction errors (MCPEs) as

$$\begin{aligned}\tilde{\mathbf{x}}_j^{m|n}(k|k) &= \mathbf{x}(k) - \hat{\mathbf{x}}_j^{m|n}(k|k) \\ &= (\mathbf{I} - \mathbf{W}_j^m(k)\mathbf{H}_j)\tilde{\mathbf{x}}_j^{m|n}(k|k-1) \\ &\quad - \mathbf{W}_j^m(k)\mathbf{w}_j(k).\end{aligned} \tag{34}$$

Since the LRs are system states, the weighting of the MCEE by the mixing probabilities in equation (33) is a nonlinear function of the state variables, which can be linearized by using Jacobians (see Section IV-A). Notice in equations (33) and (34) that as long as $\mathbf{F}$ is properly matched to the target's dynamics and previous errors and noise terms are zero mean, all MCEEs are zero mean.

$$E\left[\tilde{\mathbf{x}}_j^{m|n}(k|k)\right] = \mathbf{0}. \tag{35}$$

It is evident why a target whose dynamic mode switching includes changing $\mathbf{F}$ is more difficult to analyze: because $\mathbf{F}$ is common to both terms in equation (33), it can be factored out, yielding an expression in the MCEE. This is required for recursively computing the likelihood function parameters. Switching $\mathbf{F}$ requires additional analysis and algorithmic complexity to describe the evolution of nonzero mean MCEE and is beyond the scope of this paper. The Kalman gains $\mathbf{W}_j^l(k)$ are unknown to the FC directly, but expected values can be used in their place (see Section IV-D).

Note that the MCEE are never computed at the LT (the MCE are); equations (33) and (34) are only a probabilistic analysis of the errors for the purpose of finding the likelihood function parameters. Upon linearization, the MCEEs are jointly Gaussian stationary processes (see Section IV-A).

F. The System State of the IMM Trackers

The vector of the MCEEs and LRs describes the internal behavior of two IMM trackers estimating the state of the same target for the purpose of computing the required parameters of equations (12) and (32). Conditioned on mode n, it is defined as

$$\mathbf{y}^{|n}(k) \triangleq \left[\tilde{\mathbf{x}}_1^{|n}(k|k)'\ \tilde{\mathbf{x}}_2^{|n}(k|k)'\ \omega_1^{|n}(k)\ \omega_2^{|n}(k)\right]' \tag{36}$$

with the stacked vector of errors from each sensor written for compactness as

$$\tilde{\mathbf{x}}_1^{|n}(k|k) \triangleq \left[\tilde{\mathbf{x}}_1^{1|n}(k|k)'\ \tilde{\mathbf{x}}_1^{2|n}(k|k)'\right]'. \tag{37}$$

The mean of equation (36) is (considering that the MCE have zero mean error according to Section III-E)

$$\bar{\mathbf{y}}^{|n}(k) \triangleq E\left[\mathbf{y}^{|n}(k)\right] = \left[\mathbf{0}\quad \bar{\omega}_1^{|n}(k)\quad \bar{\omega}_2^{|n}(k)\right]'. \tag{38}$$

The covariance of equation (36) is

$$\mathbf{Y}^{|n}(k) \triangleq E\left[\mathbf{y}^{|n}(k)\mathbf{y}^{|n}(k)'\right] = \begin{bmatrix}\mathbf{P}^{|n}(k) & \mathbf{0} \\ \mathbf{0} & \mathbf{\Omega}^{|n}(k)\end{bmatrix}, \tag{39}$$

where the zeros on the off-diagonal blocks are a result of the block-diagonal Jacobian and additive noise covariance to be derived in Sections IV-A and IV-B, respectively. Recursions yield $\bar{\mathbf{y}}^{|n}(k)$ and $\mathbf{Y}^{|n}(k)$, under each hypothesis $n = 1, 2$, from which the parameters of the likelihood functions, equations (12) and (32), can be computed. This will be developed in Section IV-B. These parameters are not conditioned on any previous track information, but they do require knowledge of the measurement models, the dynamic models, and the TPM.[4]

A linearized system description of two parallel IMM LTs is depicted in Fig. 1. This diagram shows the utility of the model: the white sequences, $\mathbf{v}^n(k)$ and $\mathbf{d}^{|n}(k)$, act as common inputs to both IMM subsystems, the measurement errors $\mathbf{w}_i(k)$ act as independent inputs to each IMM, and the MCEE $\tilde{\mathbf{x}}_j^m(k|k)$ and LRs $\omega_j(k)$ act as the outputs. It is the mode-conditioned, Gaussian-approximated PDF parameters of these outputs that are of interest.

IV. ALGORITHM IMPLEMENTING BAYESIAN FUSION USING IMM INSIDE INFORMATION

While the previous section discussed important preliminary fusion theory, this section develops the algorithm for fusion with IMM Inside Information.

[4]Due to the recursive algorithm, initial conditions for $\bar{\mathbf{y}}^{|n}(k)$ and $\mathbf{Y}^{|n}(k)$ do need to be provided. Standard covariance initialization methods can be used (see [4]) and the mode-conditioned mean of the LR can be initialized to zero. This can be accomplished offline.

A. The System State Transition Jacobian

From equations (33) and (34), the Jacobians of the MCPEs with respect to the previous MCEE are

$$\mathbf{J}^{\tilde{\mathbf{x}}_j^{m|n}(k+1|k)}_{\tilde{\mathbf{x}}_i^{l|n}(k|k)}(k) = \breve{\mu}_j^{lm|n}(k)\mathbf{F}\delta_{i-j}, \tag{40}$$

where δ_{i-j} is the Kronecker Delta function (i.e., the crosssensor Jacobians in equation (40) are zero).

The Jacobians of the MCPEs with respect to the previous LR, evaluated at the mean of the errors (which are zero), are zero:

$$\mathbf{J}^{\tilde{\mathbf{x}}_j^{m|n}(k+1|k)}_{\omega_j^{|n}(k)}(k) = \frac{\pi^{1m}\pi^{2m}e^{\breve{\omega}_j^{|n}}}{\pi^{1m}e^{\breve{\omega}_j^{|n}} + \pi^{2m}}\mathbf{F}E\left[\tilde{\mathbf{x}}_j^{1|n}(k|k) - \tilde{\mathbf{x}}_j^{2|n}(k|k)\right] = \mathbf{0}. \tag{41}$$

The Jacobians of the LR with respect to their previous values can be derived from equation (23). The Jacobians of the LR with respect to the previous MCE are zero since the partial derivative of the quadratic form of innovations with respect to an innovation is scaled by that innovation, which is zero mean. This is in agreement with the claim that $\mathbf{d}_j(k)$ can be treated as white, additive noise. Omitting k, the complete Jacobian is

$$\mathbf{J}^{|n} = \begin{bmatrix} \breve{\mu}_1^{11|n}\mathbf{F} & \breve{\mu}_1^{21|n}\mathbf{F} & \mathbf{0} & \mathbf{0} & \mathbf{0} \\ \breve{\mu}_1^{12|n}\mathbf{F} & \breve{\mu}_1^{22|n}\mathbf{F} & \mathbf{0} & \mathbf{0} & \mathbf{0} \\ \mathbf{0} & \mathbf{0} & \breve{\mu}_2^{11|n}\mathbf{F} & \breve{\mu}_2^{21|n}\mathbf{F} & \mathbf{0} \\ \mathbf{0} & \mathbf{0} & \breve{\mu}_2^{12|n}\mathbf{F} & \breve{\mu}_2^{22|n}\mathbf{F} & \mathbf{0} \\ \mathbf{0} & \mathbf{0} & \mathbf{0} & \mathbf{0} & \mathbf{J}^{\boldsymbol{\omega}^{|n}(k+1)}_{\boldsymbol{\omega}^{|n}(k)} \end{bmatrix} \tag{42}$$

with

$$\mathbf{J}^{\boldsymbol{\omega}^{|n}(k+1)}_{\boldsymbol{\omega}^{|n}(k)} = \begin{bmatrix} \breve{\mu}_1^{11|n} - \breve{\mu}_1^{12|n} & \mathbf{0} \\ \mathbf{0} & \breve{\mu}_2^{11|n} - \breve{\mu}_2^{12|n} \end{bmatrix} \tag{43}$$

according to equation (23).

B. Recursion for the System Mode-Conditioned Means and Covariances

Having computed $\mathbf{J}^{|n}(k)$, the linearized system description for equation (36) under mode n becomes

$$\mathbf{y}^{|n}(k+1) = \mathbf{K}(k)\mathbf{J}^{|n}(k)\mathbf{y}^{|n}(k) + \mathbf{\Gamma}(k)\mathbf{g}^{|n}(k), \tag{44}$$

with

$$\begin{aligned} \mathbf{K}(k) &\triangleq \operatorname{diag}\left(\mathbf{K}_1^1, \mathbf{K}_1^2, \mathbf{K}_2^1, \mathbf{K}_2^2\right) \\ \mathbf{K}_j^m(k) &\triangleq \mathbf{I} - \mathbf{W}_j^m(k)\mathbf{H}_j. \end{aligned} \tag{45}$$

The noise vector

$$\mathbf{g}^{|n}(k) = \left[\mathbf{v}^n(k)' \ \mathbf{w}_1(k)' \ \mathbf{w}_2(k)' \ \mathbf{d}(k)'\right]' \tag{46}$$

has mean

$$\bar{\mathbf{g}}^{|n}(k) = E\left[\mathbf{g}(k) \mid M(k) = n\right] = \left[\mathbf{0} \ \bar{\mathbf{d}}^{|n}(k)'\right]', \tag{47}$$

where $\bar{\mathbf{d}}^{|n}(k)$ is defined in equation (29). The covariance of $\mathbf{g}^{|n}(k)$ is

$$\begin{aligned} \mathbf{G}^{|n}(k) &\triangleq E\left[[\mathbf{g}(k) - \bar{\mathbf{g}}^{|n}(k)][\mathbf{g}(k) - \bar{\mathbf{g}}^{|n}(k)]' \mid M(k) = n\right] \\ &= \operatorname{diag}\left[\mathbf{Q}^n, \mathbf{R}_1, \mathbf{R}_2, \mathbf{D}^{|n}(k)\right] \end{aligned} \tag{48}$$

and

$$\mathbf{\Gamma}(k) = \begin{bmatrix} \mathbf{I} - \mathbf{W}_1^1(k)\mathbf{H}_1 & \mathbf{W}_1^1(k) & \mathbf{0} & \mathbf{0} \\ \mathbf{I} - \mathbf{W}_1^2(k)\mathbf{H}_1 & \mathbf{W}_1^2(k) & \mathbf{0} & \mathbf{0} \\ \mathbf{I} - \mathbf{W}_2^1(k)\mathbf{H}_2 & \mathbf{0} & \mathbf{W}_2^1(k) & \mathbf{0} \\ \mathbf{I} - \mathbf{W}_2^2(k)\mathbf{H}_2 & \mathbf{0} & \mathbf{W}_2^2(k) & \mathbf{0} \\ \mathbf{0} & \mathbf{0} & \mathbf{0} & \mathbf{I} \end{bmatrix}. \tag{49}$$

Note that $\mathbf{K}(k)\mathbf{J}^{|n}(k)$ has eigenvalues inside the complex unit circle so the recursion should always converge. So, after $\mathbf{K}(k)$, $\mathbf{J}^{|n}(k)$, and $\mathbf{\Gamma}(k)$ are computed, the mean of the LR is updated as

$$\bar{\mathbf{y}}^{|n}(k+1) = \mathbf{K}(k)\mathbf{J}^{|n}(k)\breve{\mathbf{y}}^{|n}(k) + \mathbf{\Gamma}(k)\bar{\mathbf{g}}^{|n}(k), \tag{50}$$

where $\breve{\mathbf{y}}^{|n}(k)$ is a *mixed initial condition of the system recursion* with covariance $\breve{\mathbf{Y}}^{|n}(k)$.

The system's covariance update is

$$\begin{aligned} &\mathbf{Y}^{|n}(k+1) \\ &= \mathbf{K}(k)\mathbf{J}^{|n}(k)\breve{\mathbf{Y}}^{|n}(k)\mathbf{J}^{|n}(k)'\mathbf{K}(k)' + \mathbf{\Gamma}(k)\mathbf{G}^{|n}(k)\mathbf{\Gamma}(k)'. \end{aligned} \tag{51}$$

The first block on the diagonal of equation (51) is the covariance of the MCEE. With[5]

$$\mathbf{P}^{|n}(k+1|k) \triangleq \left[\mathbf{J}^{|n}(k)\breve{\mathbf{Y}}^{|n}(k)\mathbf{J}^{|n}(k)'\right]_1^{4N_x} \tag{52}$$

representing the covariance of the local MCPE, where only the first $4N_x$ rows and columns of $\mathbf{J}^{|n}(k)\breve{\mathbf{Y}}^{|n}(k)\mathbf{J}^{|n}(k)'$ are selected, the covariances and crosscovariances of the MCIs are computed as

$$\mathbf{S}^{|n}(k+1) = \mathbf{H}\mathbf{P}^{|n}(k+1|k)\mathbf{H}' + \mathbf{L}_{\mathbf{w}}\begin{bmatrix} \mathbf{R}_1 & \mathbf{0} \\ \mathbf{0} & \mathbf{R}_2 \end{bmatrix}\mathbf{L}_{\mathbf{w}}' \tag{53}$$

with

$$\mathbf{H} = \operatorname{diag}(\mathbf{H}_1, \mathbf{H}_1, \mathbf{H}_2, \mathbf{H}_2), \tag{54}$$

$$\mathbf{L}_{\mathbf{w}} = \begin{bmatrix} \mathbf{I} & \mathbf{I} & \mathbf{0} & \mathbf{0} \\ \mathbf{0} & \mathbf{0} & \mathbf{I} & \mathbf{I} \end{bmatrix}'. \tag{55}$$

[5]The notation $k+1|k$ used in covariances computed at the FC serves only to show that they are related to the state predictions made at the LT. It is not intended to mean that the computations at the FC are conditioned on past measurements.

C. The Mixing Process for Hypothesis Merging

Before every recursion update step (50)–(51), the hypotheses from the previous step must be merged, just as they are in the IMM estimation algorithm. In the absence of any previous observations, the time-invariant mixing probabilities are computed at the FC from the steady-state Markov chain probabilities $\mu^1_\infty, \mu^2_\infty$ as priors [4]:

$$\mu^{ln} = \frac{\pi^{ln}\mu^l_\infty}{\pi^{1n}\mu^1_\infty + \pi^{2n}\mu^2_\infty}. \tag{56}$$

With $M(k+1) = n$ the event that the next mode is n, the mixed initial conditions are

$$\check{\mathbf{y}}^{|n}(k) = E\left[\mathbf{y}(k) \mid M(k+1) = n\right] = \sum_{l=1}^{2} \mu^{ln}\bar{\mathbf{y}}^{|l}(k), \tag{57}$$

$$\begin{aligned}
&\check{\mathbf{Y}}^{|n}(k) \\
&= E\left[\left[\mathbf{y}(k) - \check{\mathbf{y}}^{|n}(k)\right]\left[\mathbf{y}(k) - \check{\mathbf{y}}^{|n}(k)\right]' \mid M(k+1) = n\right] \\
&= \sum_{l=1}^{2} \mu^{ln}\left[\mathbf{Y}^{|l}(k) + \left[\bar{\mathbf{y}}^{|l}(k) - \check{\mathbf{y}}^{|n}(k)\right]\left[\bar{\mathbf{y}}^{|l}(k) - \check{\mathbf{y}}^{|n}(k)\right]'\right].
\end{aligned} \tag{58}$$

D. Expected Values of the LT Stochastic Matrices

The local mode-conditioned innovation covariances $\mathbf{S}^m_j(k)$ and Kalman gains $\mathbf{W}^m_j(k)$ are required for equations (27), (45), and (49). To proceed, it should be first noted that both $\mathbf{S}^m_j(k)$ and $\mathbf{W}^m_j(k)$ are stochastic matrices, computed from a mixed covariance matrix that includes the spread-of-the-means (SOM) of the Gaussian mixture. The SOM results in a covariance update that is measurement-dependent [4]. Because the local MCE and mode probabilities depend on these stochastic matrices, the covariances as computed by the LT IMM algorithm behave like "state variables" of the system and are recursively updated. The expected value of each matrix can be computed through linearization, mixing, and recursion, then treating the resulting matrices as having zero variance (see Appendix: Property 8). This can be accomplished by expanding the FC recursion process to include finding the matrix means of the mixed initial condition covariances $\bar{\check{\mathbf{P}}}^m_j(k-1|k-1)$ and using them to find $\bar{\mathbf{S}}^m_j(k)$ and $\bar{\mathbf{W}}^m_j(k)$ using standard Kalman equations.

First, it is noted that mixed initial conditions $\check{\mathbf{x}}^m_j(k|k)$ and $\check{\mathbf{P}}^m_j(k|k)$ do not depend on the state or mode at $k+1$. Then, the recursion for the matrix mean of the local mixed initial condition matrix can be linearized as

$$\begin{aligned}
\bar{\check{\mathbf{P}}}^m_j(k|k) &\triangleq E\left[\check{\mathbf{P}}^m_j(k|k)\right] \\
&= E\left\{\sum_{l=1}^{2} \mu^{lm}_j(k)\left[\mathbf{P}^l_j(k|k) + \mathbf{N}(k)\right]\right\} \\
&= \sum_{n=1}^{2} E\left\{\sum_{l=1}^{2} \mu^{lm}_j(k)\Big[\mathbf{P}^l_j(k|k) \right. \\
&\qquad \left. + \mathbf{N}^{lm}_j(k) \mid M(k) = n\Big]\right\} \cdot P\left[M(k) = n\right] \\
&\approx \sum_{n=1}^{2}\Big[\sum_{l=1}^{2} \check{\mu}^{lm|n}_j(k) E\left[\mathbf{P}^l_j(k|k) \mid M(k) = n\right] \\
&\qquad + \check{\mu}^{lm|n}_j(k) E\left[\mathbf{N}^{lm}_j(k) \mid M(k) = n\right]\Big]\mu^n_\infty.
\end{aligned} \tag{59}$$

In equation (59), $\mu^{lm}_j(k)$ can be taken out of the expectation (as a first-order linear approximation) and evaluated using $\check{\omega}^{|n}_j(k)$ and equation (24); $\mathbf{N}^{lm}_j(k)$ is the SOM. The expectation in the first term can be computed by

$$\begin{aligned}
\bar{\mathbf{P}}^l_j(k|k) &\triangleq E\left[\mathbf{P}^l_j(k|k) \mid M(k) = n\right] = E\left[\mathbf{P}^l_j(k|k)\right] \\
&= \mathbf{F}\bar{\check{\mathbf{P}}}^l_j(k-1|k-1)\mathbf{F}' + \mathbf{Q}^l - \mathbf{W}^l_j(k)\mathbf{S}^l_j(k)\mathbf{W}^l_j(k)'.
\end{aligned} \tag{60}$$

Omitting the step k, the expected value of the SOM can be derived starting with

$$\begin{aligned}
&E\left[\mathbf{N}^{lm}_j \mid M(k) = n\right] \\
&\qquad = E\left[\left[\hat{\mathbf{x}}^l_j - \check{\mathbf{x}}^m_j\right]\left[\hat{\mathbf{x}}^l_j - \check{\mathbf{x}}^m_j\right]' \mid M(k) = n\right]
\end{aligned} \tag{61}$$

and expanding the difference as

$$\begin{aligned}
\hat{\mathbf{x}}^l_j - \check{\mathbf{x}}^m_j &= \hat{\mathbf{x}}^l_j - \sum_{o=1}^{2} \mu^{om}_j \hat{\mathbf{x}}^o_j \\
&= \begin{cases} \mu^{2m}_j\left[\hat{\mathbf{x}}^1_j - \hat{\mathbf{x}}^2_j\right] & \text{if } l = 1 \\ \mu^{1m}_j\left[\hat{\mathbf{x}}^2_j - \hat{\mathbf{x}}^1_j\right] & \text{if } l = 2. \end{cases}
\end{aligned} \tag{62}$$

Since the two MCEs have the same mean, $\mathbf{x}$,

$$\begin{aligned}
&E\left[\mathbf{N}^{lm}_j \mid M(k) = n\right] \\
&= \begin{cases} (\check{\mu}^{2m}_j)^2\left(\mathbf{P}^{11|n}_{jj} + \mathbf{P}^{22|n}_{jj} - \mathbf{P}^{12|n}_{jj} - \mathbf{P}^{21|n}_{jj}\right) & \text{if } l = 1 \\ (\check{\mu}^{1m}_j)^2\left(\mathbf{P}^{11|n}_{jj} + \mathbf{P}^{22|n}_{jj} - \mathbf{P}^{12|n}_{jj} - \mathbf{P}^{21|n}_{jj}\right) & \text{if } l = 2 \end{cases}
\end{aligned} \tag{63}$$

where each $\mathbf{P}^{lm|n}_{jj}$ is a respective block of equation (14). Finally, after computing $\bar{\check{\mathbf{P}}}^m_j(k-1|k-1)$ using equations

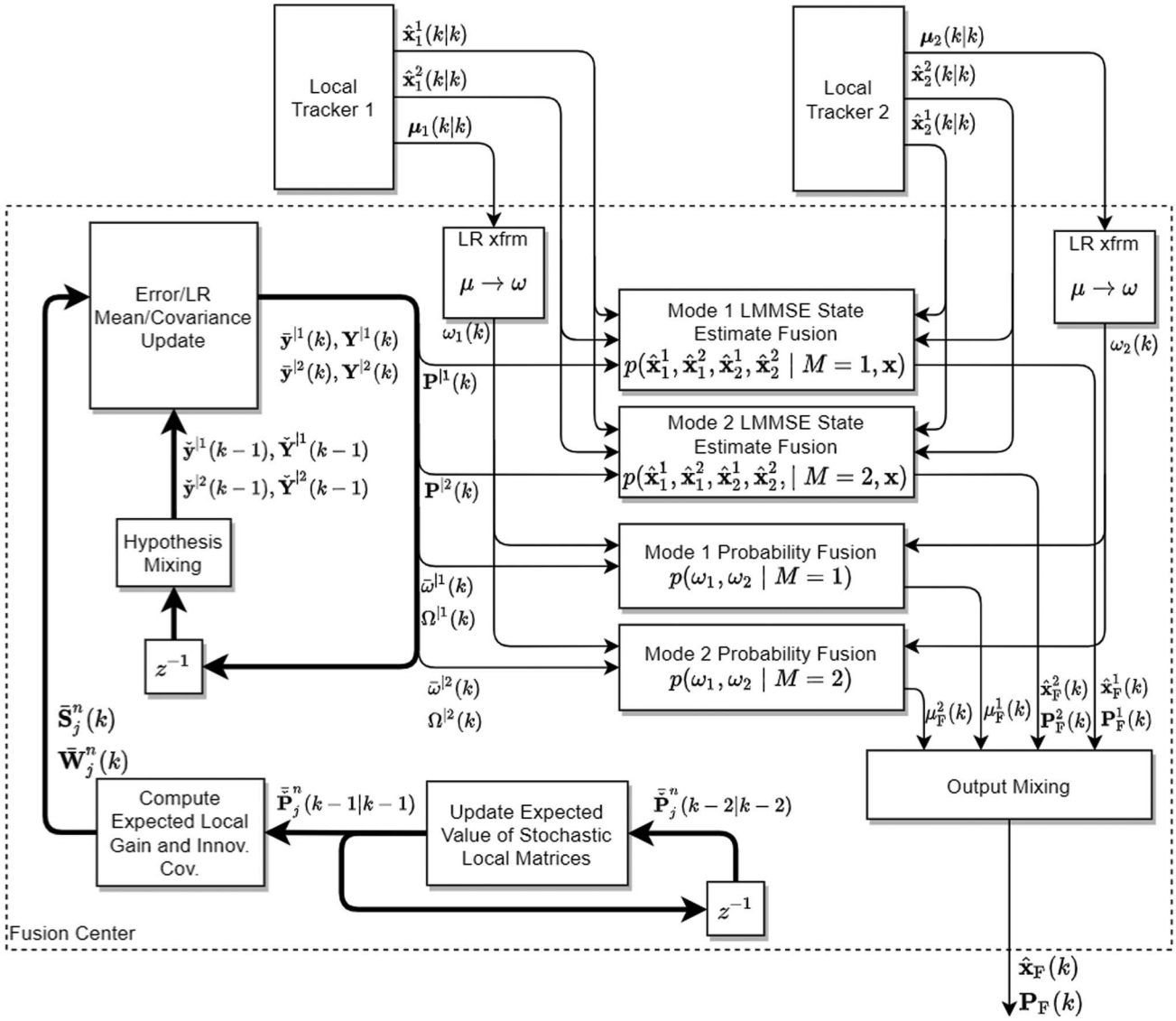

Fig. 2. Block diagram of the proposed IMM inside information fusion algorithm. $\bar{\omega}^{|n}$ is part of $\mathbf{y}^{|n}$ and $\mathbf{Y}^{|n}$ is block-diagonal with $\mathbf{P}^{|n}$ and $\mathbf{\Omega}^{|n}$ as its respective blocks. The relevant Gaussian likelihood functions used for fusion are shown in the fusion blocks.

(59), (60), and (63), the required expected values of the stochastic matrices can be computed as

$$\bar{\mathbf{P}}_j^m(k|k-1) = \mathbf{F}\bar{\bar{\mathbf{P}}}_j^m(k-1|k-1)\mathbf{F}' + \mathbf{Q}^m, \tag{64}$$

$$\bar{\mathbf{S}}_j^m(k) = \mathbf{H}_j\bar{\mathbf{P}}_j^m(k|k-1)\mathbf{H}_j' + \mathbf{R}_j, \tag{65}$$

$$\bar{\mathbf{W}}_j^m(k) = \bar{\mathbf{P}}_j^m(k|k-1)\mathbf{H}_j'\bar{\mathbf{S}}_j^m(k)^{-1}. \tag{66}$$

E. The Fused Estimate and Covariance Output

Omitting k for brevity, the fused estimate of the target state, in the minimum MSE sense, is the mean of the posterior fused mixture (9):

$$\hat{\mathbf{x}}_{\mathrm{F}} = \sum_{n=1}^{2} \mu_{\mathrm{F}}^n \hat{\mathbf{x}}_{\mathrm{F}}^n \tag{67}$$

and has expected MSE

$$\mathbf{P}_{\mathrm{F}} = \sum_{n=1}^{2} \mu_{\mathrm{F}}^n \left[\mathbf{P}_{\mathrm{F}}^n + (\hat{\mathbf{x}}_{\mathrm{F}}^n - \hat{\mathbf{x}}_{\mathrm{F}})(\hat{\mathbf{x}}_{\mathrm{F}}^n - \hat{\mathbf{x}}_{\mathrm{F}})'\right]. \tag{68}$$

V. SUMMARY

A. Algorithmic Steps

A block diagram of the overall fusion method is depicted in Fig. 2. The outside information fusion, which fuses the moment-matched IMM outputs, is depicted in Fig. 3 for comparison.

The algorithm can be interpreted as an IMM combined with an extended Kalman filter (EKF) whose recursion is executed without track data. The goal of the recursion is to compute the mode-conditioned covariance/crosscovariance matrix of the MCE (conditioned on $\mathbf{x}$) and the mode-conditioned mean plus

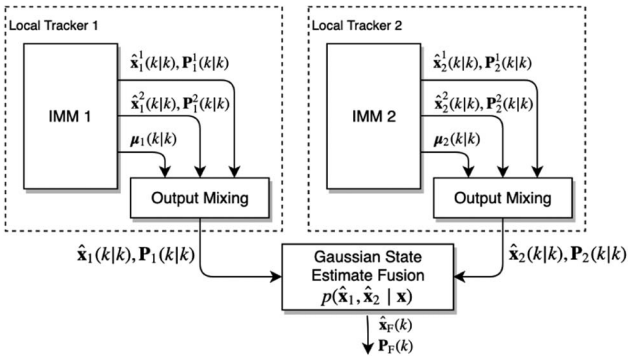

Fig. 3. Block diagram of conventional outside fusion method. The Gaussian likelihood function used is written in the fusion block.

covariance/crosscovariance matrix of the LR to be used in the fusion process when the data arrive. The state variables of the EKF/IMM-like algorithm are considered to be the MCEE $\tilde{\mathbf{x}}_j^m$, LR ω_j, and the the local covariance matrices $\mathbf{P}_j^m$ (where only the mode-conditioned mean of the components of the latter matrices is computed). The steps are as follows.

For $n = 1, 2$, initialize the following:

1) Set $\bar{\omega}_1^{|n}(0) \leftarrow 0, \bar{\omega}_2^{|n}(0) \leftarrow 0$.
2) $\mathbf{\Omega}^{|n}(0) \leftarrow c\mathbf{I}$ (where c should be large enough to cover the expected error — see [4]; a value of 1 is used in the simulations of Section VI).
3) Diagonal blocks of $\mathbf{P}^{|n}(0)$ (the covariances of the MCEE) are initialized the same as LT (see [4]), or using $c\mathbf{I}$, where c is large enough to cover the expected errors.
4) The off-diagonal blocks of $\mathbf{P}^{|n}(0)$ are initialized with zeros (i.e., the crosscovariances can be initialized to zero).
5) The expected values of the hidden local mixed initial condition matrices $\bar{\mathbf{P}}_j^n(0|0)$, for $j = 1, 2$, are initialized the same as LT and the diagonal blocks of $\mathbf{P}^{|n}(0)$.
6) Compute steady-state Markov chain probabilities μ_∞^n.
7) Set $k = 1$.

Repeat the following for each k (synchronously with LT or offline) for $j = 1, 2, l = 1, 2, m = 1, 2$, and $n = 1, 2$:

1) Mixing: Compute $\check{\mathbf{y}}^{|n}(k-1)$ and $\check{\mathbf{Y}}^{|n}(k-1)$ using equations (57) and (58).
2) Compute $\check{\mu}_j^{lm|n}(k-1)$ using equation (24) (substitute $\check{\omega}_j^{|n}(k-1)$ for $\omega_j^{|n}(k-1)$).
3) Compute the mean of the local mixed initial condition matrices $\bar{\tilde{\mathbf{P}}}_j^m(k-1|k-1)$ using equation (59).
4) Compute the expected value of the local $\bar{\mathbf{S}}_j^m(k)$ and $\bar{\mathbf{W}}_j^m(k)$ using equations (64), (65) and (66).
5) Compute joint system state mean $\bar{\mathbf{y}}^{|n}(k)$ using equation (50).
6) Compute joint system state covar $\mathbf{Y}^{|n}(k)$ using equation (51).

If LT data (10) arrive at time step k, then for $n = 1, 2$:

1) extract $\bar{\omega}_1^{|n}, j = 1, 2$, from $\bar{\mathbf{y}}^{|n}(k)$ and $\mathbf{P}^{|n}(k)$, $\mathbf{\Omega}^{|n}(k)$ from $\mathbf{Y}^{|n}(k)$. See equation (38) and (39);
2) compute fused MCE $\hat{\mathbf{x}}_F^n(k)$ using equation (15);
3) compute fused MCC $\mathbf{P}_F^n(k)$ using equation (16);
4) compute fused mode probabilities $\mu_F^n(k)$ using equation (31);
5) compute output mean $\hat{\mathbf{x}}_F(k)$ and MSE $\mathbf{P}_F(k)$ using equations (67) and (68).

B. Computational Complexity

The algorithm described in this paper consists of two main routines, which are both computationally feasible for real-time performance. The first is the recursive computation of $\bar{\mathbf{y}}^{|n}(k)$, $\mathbf{Y}^{|n}(k)$ and the hidden stochastic matrices $\bar{\mathbf{S}}_j^m(k)$ and $\bar{\mathbf{W}}_j^m(k)$. This algorithm is analogous to an IMM track predictor with EKF mode predictors (i.e., an IMM with no data). Since this paper does not explicitly generalize the algorithm to more than two modes and two LTs, the order of complexity will be discussed in terms of the state dimension N_x only. It can be seen in equations (57) and (58) that there are $2^2 = 4$ mixing operations as in a two-mode IMM, where each mixing operation scales quadratically with N_x due to the outer product of equation (58). Each mode is approximately on the order of $O[(2 \cdot 2N_x)^2]$ due to the FC's EKF-like prediction recursion (50), (51). The hidden matrix computations (59)–(66), where a matrix inversion is involved, scale approximately as $O[2 \cdot 2N_x^3]$, so the overall computational order is $O[N_x^3]$. Since the target and LT parameters are time-invariant, these recursive computations can be performed offline.

The second routine is the actual fusion of the data when they arrive. Since Gaussian LMMSE fusion is performed for each mode (see equations (15) and (16)) and matrix inversion dominates the order, its complexity scales approximately as $O[N_x^3]$.

Chernoff fusion scales similarly for each selection of the fusion exponent w due to the matrix inversion of the least-squares parameter estimation [8]. The search for the optimal w using a grid of N_w values on the interval (0,1) means that the sigma point Chernoff fusion method of [8] scales approximately as $O[N_w N_x^3]$.

VI. SIMULATION RESULTS

The simulations have the local IMM estimators tracking a target in 2D space observed by sensors that are measuring its Cartesian position. Two LTs run IMM estimators and use two dynamic modes described in the sequel. Three scenarios are considered: the first has a deterministic target trajectory (ground truth) using a

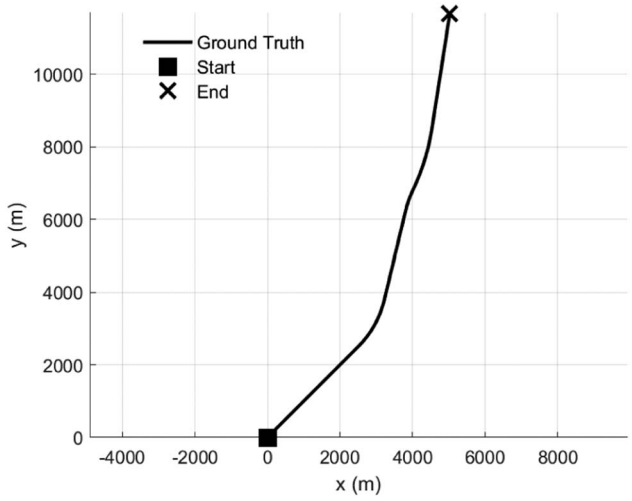

Fig. 4. The fixed target trajectory of the first scenario.

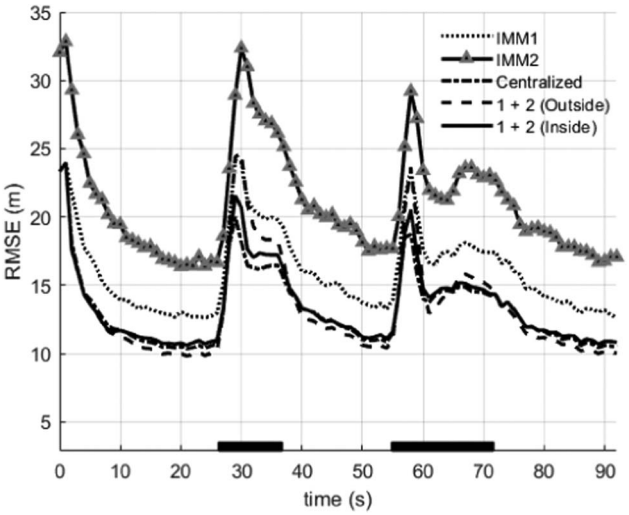

Fig. 5. Position RMSE of local IMMs, CMF, outside fusion, and inside fusion.

coordinated-turn model (see [4]) and fusion at full rate; the second has the same deterministic trajectory with fusion at a reduced rate (as a sanity check since the proposed method's performance at fusion times is not affected by fusion rate); and the third simulates random trajectories driven by white noise, with a dynamic model matching that of the estimators and with fusion at full rate.

A. Ground Truth

The measurement interval is $T = 1\,\text{s}$. The target starts at $x = 0, y = 0$ with $\dot{x} = 100\,\text{m/s}, \dot{y} = 100\,\text{m/s}$. The target:

1) travels straight for 25.2 s;
2) performs a constant-rate left turn of $3\,^\circ/\text{s}$ for 10.6 s;
3) travels straight for 18 s;
4) performs a constant-rate right turn of $-3\,^\circ/\text{s}$ for 4.1 s;
5) performs a constant-rate left turn of $1.3\,^\circ/\text{s}$ 12.8 s;
6) travels straight for 22.6 s.

A plot of this constant-speed, variable-turn rate trajectory is shown in Fig. 4.

B. Estimation Models

The state vector is composed of stacked position and velocity

$$\mathbf{x}(k) = [x(k)\; y(k)\; \dot{x}(k)\; \dot{y}(k)]'. \tag{69}$$

The estimator dynamic models are described as follows. Mode 1 is a 2D WNA model, discretized from the continuous-time model [4]. It has a 2D process noise acceleration with intensity (power spectral density) $\tilde{q}^1 = 0.01^2\,\text{m}^2/\text{s}^3$, and Mode 2 is the same but with $\tilde{q}^2 = 7.5^2\,\text{m}^2/\text{s}^3$:

$$\mathbf{F} = \begin{bmatrix} 1 & 0 & T & 0 \\ 0 & 1 & 0 & T \\ 0 & 0 & 1 & 0 \\ 0 & 0 & 0 & 1 \end{bmatrix}, \tag{70}$$

$$\mathbf{Q}^n = \begin{bmatrix} \frac{1}{3}T^3 & 0 & \frac{1}{2}T^2 & 0 \\ 0 & \frac{1}{3}T^3 & 0 & \frac{1}{2}T^2 \\ \frac{1}{2}T^2 & 0 & T & 0 \\ 0 & \frac{1}{2}T^2 & 0 & T \end{bmatrix} \tilde{q}^n. \tag{71}$$

The TPM is

$$\Pi = \begin{bmatrix} 0.95 & 0.05 \\ 0.05 & 0.95 \end{bmatrix}. \tag{72}$$

The measurement parameters are

$$\mathbf{H}_1 = \mathbf{H}_2 = \begin{bmatrix} 1 & 0 & 0 & 0 \\ 0 & 1 & 0 & 0 \end{bmatrix}, \tag{73}$$

$$\mathbf{R}_1 = \text{diag}[(15\,\text{m})^2, (18\,\text{m})^2], \tag{74}$$

$$\mathbf{R}_2 = \text{diag}[(20\,\text{m})^2, (25\,\text{m})^2]. \tag{75}$$

C. Fusion Results

Figs. 5 and 6 show the position and velocity RMSE for the inside information fusion, outside information fusion (naive Gaussian fusion with no crosscovariances), and CMF methods, along with the RMSE of the local sensor tracks. The inside fusion is slightly outperformed by the outside fusion during straight-line motion, just as the centralized fusion is, but inside fusion significantly outperforms outside fusion during maneuvers. It is interesting to note the low RMSE during

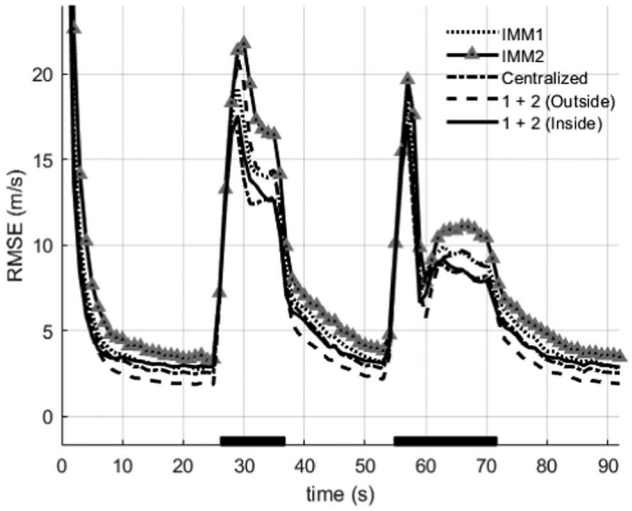

Fig. 6. Velocity RMSE of local IMMs, CMF, outside fusion, and inside fusion.

straight-line motion for naive outside fusion and that it outperforms the method of this paper and CMF during these times. This is explained by the fact that outside fusion computes a small covariance matrix that significantly reduces the overall filter "bandwidth" [4], but because of this, it performs very poorly during maneuvers (i.e., it does not minimize the maximum error). Section VI-E performs simulations with Monte Carlo randomly generated trajectories that match the stochastic model of the target, and those simulations show that, on average, CMF and the fusion with IMM inside information do indeed outperform naive outside fusion.

The consistency is evaluated using the normalized estimation error squared (NEES, see [4]), divided by N_x (the state dimension) and this is plotted for every time point in Fig. 7. Values near 1 are ideal and reflect a chi-square quadratic form resulting from estimation errors

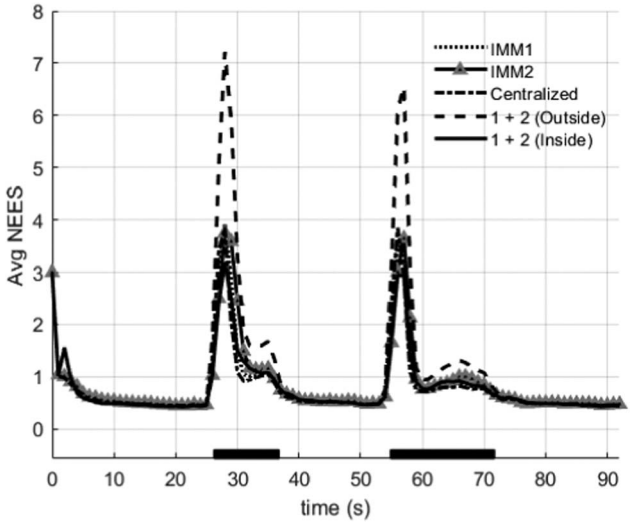

Fig. 7. NEES of local IMMs, CMF, outside fusion, and inside-information fusion. Value is normalized by N_x to be 1 when fused covariance matches sample MSE.

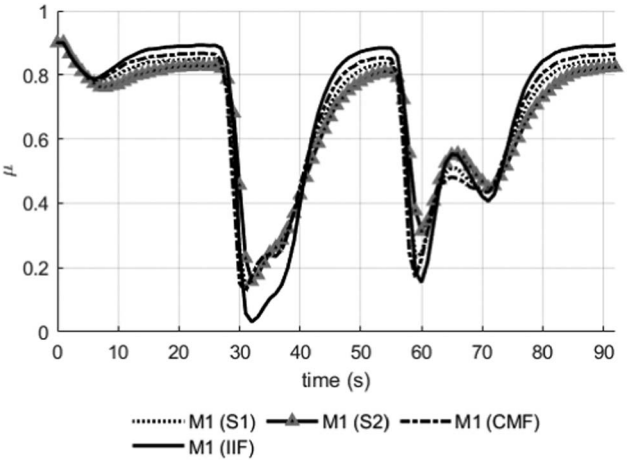

Fig. 8. Computed probability of mode 1 from local IMMs (S1, S2), inside information-fusion, and CMF.

that are zero mean and consistent with the state covariances. It is clear that the inside-information method achieves better consistency.

In Fig. 8, the mode probabilities of the inside-information fusion are compared to the local IMM mode probabilities and the CMF mode probabilities. The fused mode probabilities computed by the inside-information fusion slightly lead the probabilities of the local sensors when transitioning modes and, so, maneuvers can be detected quicker than they can be at the LT. Although the transient performance is encouraging, it can also be seen that the method as described in this paper results in fused mode probabilities that are "more sure" about the mode—centralized fusion is more conservative and only boosts this conviction slightly.

D. Reduced-Rate Fusion

As a sanity check, it should be shown that fusion performance is not affected by the rate at which track data are transmitted. An advantage to the T2TF using inside information presented here is that it is not affected by previous tracks. Outside information fusion is known not to be affected by fusion rate because it utilizes the standard Gaussian fusion method without memory. As can be seen in Fig. 2, the LR mean/covariance and the MCEE covariance (including crosscovariances between trackers) are recursively updated whether there is track information or not, and received tracks are not used in that computation (in the scenario presented here, $\bar{\mathbf{y}}^{|n}$ and $\mathbf{Y}^{|n}$ can even be computed offline).

Figs. 9–11 show the comparison of outside information fusion to the inside information fusion at a reduced rate of once every five measurement intervals, starting at $k = 4$. Looking closely, the performance at the fusion times matches the performance shown in Figs. 5–7. Again, it can be seen that the inside information fusion, like CMF, only outperforms outside information fusion during maneuvers, but the consistency of the fused covariance is significantly superior for inside-information

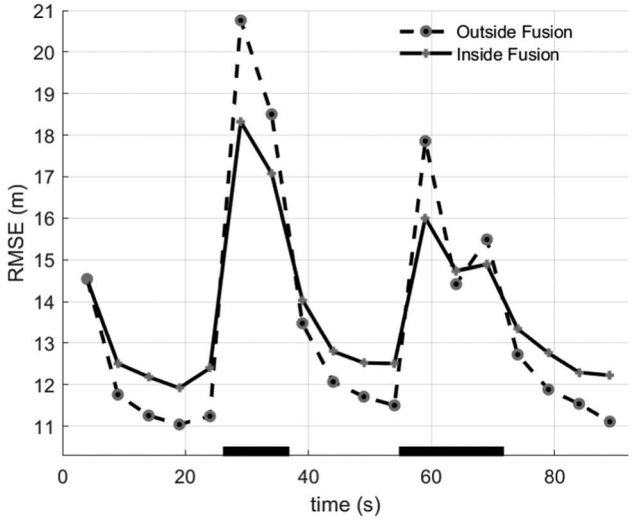

Fig. 9. Position RMSE of outside information fusion and inside information fusion at reduced rate, fusing tracks once every five measurement intervals.

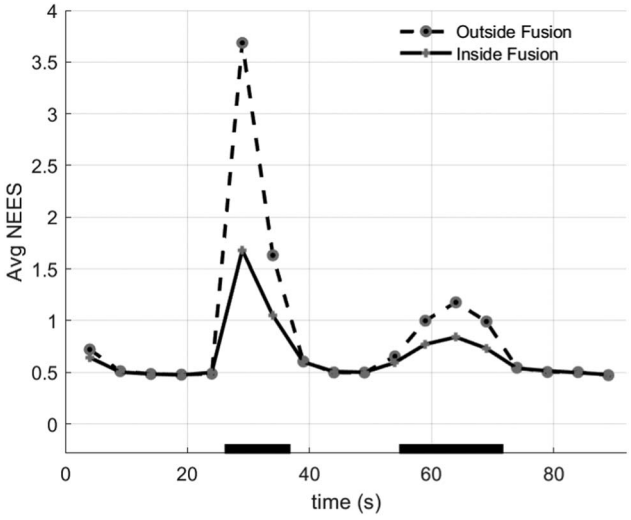

Fig. 11. NEES of outside information fusion and inside information fusion at reduced rate, fusing tracks once every five measurement intervals.

fusion. The next section demonstrates that, on average, CMF and fusion with inside information are actually more accurate.

E. Simulations Using Random, Model-Matched Target Trajectories

While the simulations of the previous sections were carried out using a single realization of the true target trajectory, the trajectory simulations of this section are randomized for every Monte Carlo run. This provides a better comparison of the overall behavior of the algorithms and highlights the consistency of the inside-information fusion.

The random trajectories are created using the WNA model driven by zero mean white noise having covariance given in equation (71).[6] The mode n is selected according to realizations of the Markov chain having TPM (72). The results are shown in Figs. 12–14. It can be seen that the position RMSE is close to equal for CMF, outside fusion, and inside fusion. Fusion with outside information has more velocity RMSE. Due to the matched target and estimator parameters, the NEES, normalized to nominal one, measures the overall MSE consistency of the IMM trackers (where CMF is simply an IMM with stacked measurement vectors). Fusion with inside information can be seen to be as consistent as centralized fusion, demonstrating that it is a fusion that accounts for error correlations (i.e., the crosscovariances) and provides a consistent fused covariance output. Outside-information fusion has NEES that is 50% higher than the ideal NEES of inside-information fusion meaning that the fused estimate covariance from outside fusion is, on average, 33% smaller than it should be given the actual sample error covariance.

Figs. 12–14 also show the results of Chernoff fusion using the sigma-point method of [8], where the weight parameter is searched at every time step in the interval [0.01, 0.99] using increments of 0.01. It can be seen that although the Chernoff fused covariance closely matches the actual sample MSE of the fused estimate (according to the NEES), its RMSE is higher than both inside-information and outside-information fusion. So in this application, the MSE consistency of Chernoff fusion is evident, but its inability to incorporate the known system parameters renders it more inaccurate than the model-based fusion using IMM inside information. On average, fusion with IMM inside information performed

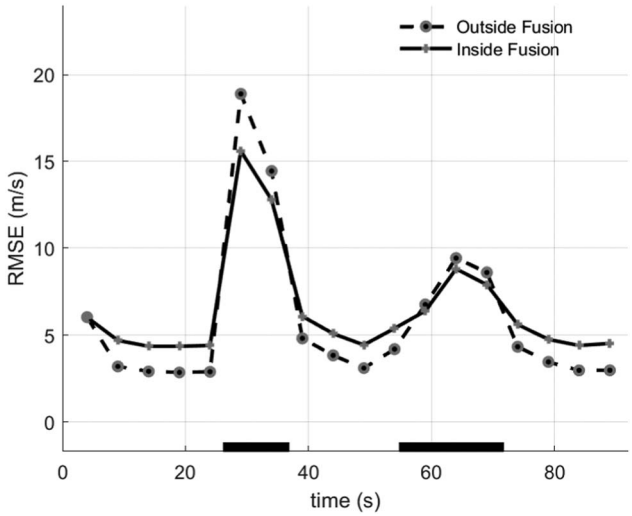

Fig. 10. Velocity RMSE of outside information fusion and inside information fusion at reduced rate, fusing tracks once every five measurement intervals.

[6]White noise is a requirement for the state of the system to be a Markov process, which is a requirement for the existence of an estimator [4].

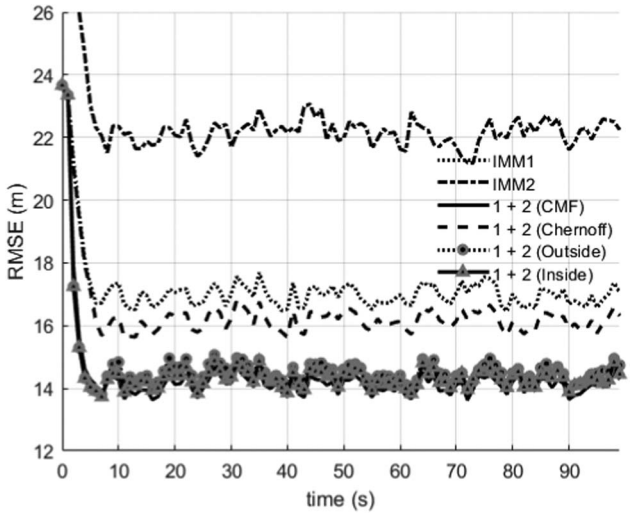

Fig. 12. Position RMSE of local IMMs, CMF, Chernoff fusion, outside fusion, and inside fusion, using random, model-matched target trajectories.

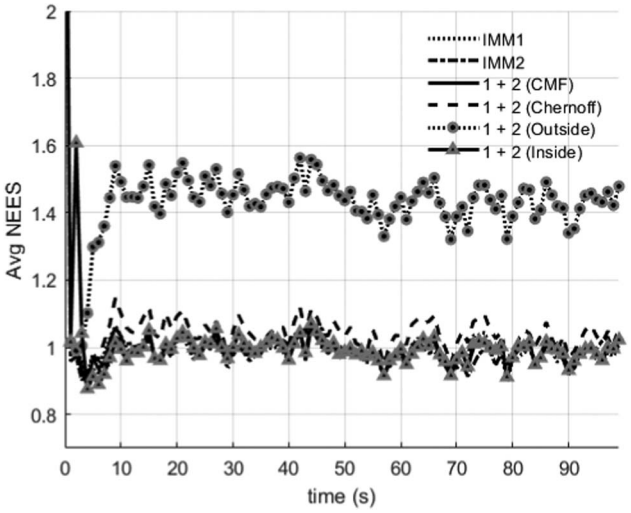

Fig. 14. NEES of local IMMs, CMF, Chernoff fusion, outside fusion, and inside fusion, using random, model-matched target trajectories. All estimators, except outside fusion, achieve ideal consistency of the MSE.

approximately 100 times faster than Chernoff fusion (see Section V-B for complexity analysis).

VII. CONCLUSIONS

A system model of two IMM trackers estimating the state of a maneuvering target was presented for T2TF using information from inside the local IMM estimators. The fusion estimator produces a posterior fused mean and covariance that is reduced from a Gaussian mixture. The mixture parameters are computed from IMM track information from two LTs, with the target modeled as jumping between two dynamic modes. The linearized system model, together with the LR transformation of the received mode probabilities, yields covariances and crosscovariances of the local mode-conditioned errors, and also yields the mode-conditioned means, variances, and covariances of the scalar LRs. From these, the parameters of the likelihood functions of the mode-conditioned state and the mode are derived. Each fused mode-conditioned state estimate uses information from all received MCE. The result is on-demand Bayesian fusion capability with no previous fused track information needed. Compared to the naive fusion of moment-matched Gaussian track information (i.e., outside information fusion), the new method achieves performance closer to the CMF method and outperforms the naive fusion in both RMSE and covariance consistency, most notably when the target is in a maneuvering mode. Fusion with inside information was shown to be consistent on average as it accounts for the crosscovariance of the local estimate errors and mode probabilities, whereas fusion with outside information and no crosscovariance has a computed covariance that is 33% too small on average. Compared to Chernoff fusion, the method is more accurate, consistent, provides mode inference, and is computationally faster.

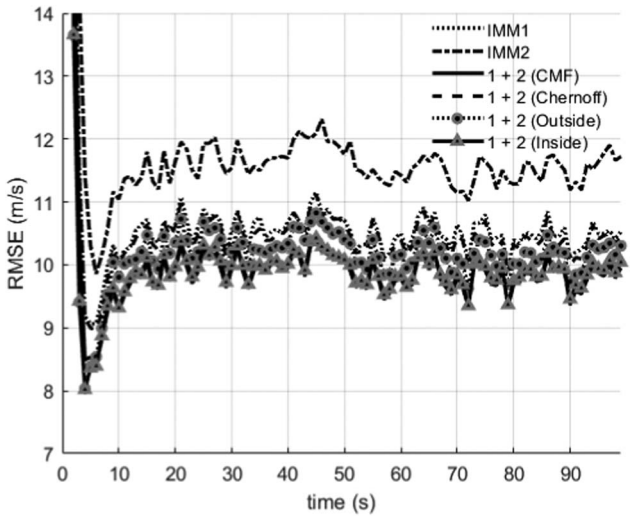

Fig. 13. Velocity RMSE of local IMMs, CMF, Chernoff fusion, outside fusion, and inside fusion, using random, model-matched target trajectories.

APPENDIX CORRELATION, DEPENDENCY, AND STATISTICAL INFORMATION PROPERTIES

The following properties of the LT track parameters and fused estimates establish some of the claims made in this paper. For jointly Gaussian densities, uncorrelated random variables are independent. Equivalently, if there is no linear dependency among them, then the variables are uncorrelated. The following claims are proved under the multiple model, linear-Gaussian approximation (Property 4 is proved without approximation):

Property 1: *The locally computed, mode-conditioned innovations are zero mean and wide-sense white sequences regardless of the true target mode*. First, it is noted that since the **F** is the same for both modes and

the process noise is zero mean, all MCEE and innovations are zero mean (see Section III-E). The whiteness proof for single-mode systems is given in [4] using the smoothing property of expectations. The following generalizes that proof because conditioning on mode $M(k)$ does not change this result. Let $k_1 < k_2$, then

$$\begin{aligned} &E\left[\boldsymbol{\nu}_j^m(k_2)\boldsymbol{\nu}_j^m(k_1)' \mid M(k_2)=n\right] \\ &\quad = E\left[E\left[\boldsymbol{\nu}_j^m(k_2)\boldsymbol{\nu}_j^m(k_1)' \mid \mathbf{Z}_j^{k_2-1}\right] \mid M(k_2)=n\right] \\ &\quad = E\left[E\left[\boldsymbol{\nu}_j^m(k_2) \mid \mathbf{Z}_j^{k_2-1}\right]\boldsymbol{\nu}_j^m(k_1)' \mid M(k_2)=n\right] \\ &\quad = \mathbf{S}_j^m(k_2)\delta_{k_2-k_1} \end{aligned} \tag{A1}$$

Property 2: *The LRs of the local mode probabilities are orthogonal to the local MCEEs*. Under the multiple-model, linear-Gaussian approximation, the LR evolve as a Markov process (22) driven by white noise that is uncorrelated to the noise that drives the MCEE process. In Section III-C, the LR Gaussian white noise $\mathbf{d}(k)$ is approximated from the quadratic form of the innovations. Likewise, conditioned on the target dynamic mode, the MCEE evolve as a Markov process according to equations (33) and (34), where their additive white noise is a linear combination of the process noise and the measurement noise. Since the covariance between a vector and its quadratic form is zero, the additive noises of the LR and MCEE are uncorrelated. Additionally, the Jacobian (42) is block-diagonal, where the MCEE do not linearly depend on previous values of the LR and vice-versa.

Property 3: *Given the LT MCEs, the LRs of the received mode probabilities do not contribute additional information about the mode-conditioned target state*. Using the principle of orthogonality [4], this is written as

$$E\left\{\begin{bmatrix}\omega_1(k)\\ \omega_2(k)\end{bmatrix}\tilde{\mathbf{x}}_{\mathrm{F}}^n(k)' \mid M(k)=n\right\} = \mathbf{0}. \tag{A2}$$

This holds because $\tilde{\mathbf{x}}_{\mathrm{F}}^n(k)$ is a linear combination of the MCEE $\tilde{\mathbf{x}}_j^m(k)$, $m = 1, 2$, $j = 1, 2$ according to equation (15). Because of Property 2 and this linear combination, $\tilde{\mathbf{x}}_{\mathrm{F}}^n(k)$ is also orthogonal to the LR.

Property 4: *The received MCE do not contain information about the target's mode probability.* This can be proved without the linear-Gaussian approximation using the fact that the likelihood of the mode based on the received MCE is a diffuse (noninformative) PDF; the state vector is composed of integrated (i.e., nonstationary) position and velocity:

$$p[\hat{\mathbf{x}}_1^1, \hat{\mathbf{x}}_1^2, \hat{\mathbf{x}}_2^1, \hat{\mathbf{x}}_2^2 \mid M=m] \to 0, \quad m = 1, 2, \tag{A3}$$

for any values of the MCE. Note that this property is not necessarily satisfied if the state vector contains stationary process(es), e.g., discretized Ornstein–Uhlembeck acceleration, autoregressive processes, or if the $\mathbf{F}$ matrix switches with the mode.

Property 5: *The components of the MCEE covariance matrices are orthogonal to the MCEEs and the LRs.* In any single-mode linear-Gaussian system, this is easily proved since the computed state covariance matrix does not depend on the observations. Let $q_j^{l(n,o)}(k) = q_j^{l(o,n)}(k)$ denote the locally computed scalar error covariance of the n-th and o-th state components (i.e., the n-th, o-th and the o-th, n-th components of $\mathbf{P}_j^l(k|k)$ as computed by the jth IMM estimator). This quantity is understood to be the covariance of the error of the l-th MCE conditioned on LT measurements up to k and target mode l being in effect. It can be stated as

$$q_j^{l(n,o)}(k) \triangleq E\left[\tilde{x}^{l(n)}(k)\tilde{x}(k)^{l(o)} \mid \mathbf{Z}_j^k, M(k)=l\right]. \tag{A4}$$

Conditioned on mode n at the FC, the first correlation to be analyzed is that of $q_j^{l(n,o)}(k)$ and any MCEE $\tilde{\mathbf{x}}_j^p(k)$. Since any zero mean Gaussian random variable is uncorrelated to the product of any other two Gaussian random variables,

$$\begin{aligned} &E\left[q_j^{l(n,o)}(k)\tilde{\mathbf{x}}_j^p(k) \mid M(k)=n\right] \\ &\quad = E\Bigg[E\left[\tilde{x}^{l(n)}(k)\tilde{x}^{l(n)}(k) \mid \mathbf{Z}_j^k, M(k)=l\right] \\ &\qquad \cdot \tilde{\mathbf{x}}_j^p(k) \mid M(k)=n\Bigg] \\ &\quad = \mathbf{0}, \end{aligned} \tag{A5}$$

and similar analysis can be used to also prove the lack of correlation between $q_j^{l(n,o)}(k)$ and $[\omega_1(k), \omega_2(k)]'$.

Property 6: *Given the LT MCEs, the received covariance components $q_j^{l(n,o)}(k)$ do not contain any linearly dependent information about the mode-conditioned target state $\mathbf{x}^{|n}(k)$*. This can be proved using the principle of orthogonality: the fused mode-conditioned target state estimate error $\tilde{\mathbf{x}}_{\mathrm{F}}^n(k)$ is a linear combination of the MCEE, which are uncorrelated to $q_j^{l(n,o)}(k)$ according to Property 5.

Property 7: *The received covariance components $q_j^{l(n,o)}(k)$ do not contain significant information about the target dynamic mode $M(k)$ or the mode-conditioned target state $\mathbf{x}^{|n}(k)$*. Because of the nonlinear operations involved in computing $\mathbf{P}_j^l(k|k)$, it is difficult to prove this. However, an approximate argument can be made based on the nature and intention of the IMM estimator. First, it is stated in Section IV-D that the MCC do not depend on the state or measurements at the current time step, so not much information should be expected. They do, however, depend on the previous MCE and mode probabilities because of the SOM matrix term. But the SOM is only a result of the mixing process that prevents the exponential growth of mode history hypotheses, and this method allows for feasible, yet suboptimal, multiple-model estimation. Certainly, in single-mode Gaussian

systems, or when using the infeasible optimal multiple-model estimator [4], covariance/crosscovariance matrices are deterministic, carry no statistical information, and can be easily computed at the FC. For example, this can be easily seen in the special case where the target is known to be in a specific state at the previous time step: there is no SOM in this case.

If system designers do not have access to LT design parameters or the target motion parameters, then it makes sense why received covariance matrices would be part of the fusion process. In such unfortunate scenarios, the FC must utilize a highly approximate fusion algorithm like covariance intersection or Chernoff fusion. However, knowledge of the computational pipeline of the LT track parameters allows for systematic, model-based Bayesian fusion as presented here.

Property 8: *Direct access to the locally-computed, mode-conditioned Kalman gains and innovation covariances does not improve the fused target state estimate or the consistency of the fused estimate covariance; likewise, computing and incorporating the covariance of these locally-computed covariance components does not affect the fused estimate or fused covariance*. This is a direct consequence of Property 5. It can be shown that because the components of the MCC are uncorrelated to the MCEE and the LR, then the MCEE and LR covariances are unaffected by the covariance of the LT Kalman gains and innovation covariance components. Only the mode-conditioned means of these matrices need to be computed at the FC as presented in Section IV-D.

REFERENCES

[1] D. Acar and U. Orguner
"Information decorrelation for an interacting multiple model filter,"
in *Proc. 21st Conf. on Inf. Fusion*, Jul. 2018.

[2] Y. Bar-Shalom
"On the track-to-track correlation problem,"
IEEE Trans. Automatic Control, vol. AC-26, no. 2, pp. 571–572, Apr. 1981.

[3] Y. Bar-Shalom and L. Campo
"The effect of the common process noise on the two-sensor fused-track covariance, "
IEEE Trans. Aerosp. Electron. Syst., vol. AES-22, no. 6, pp. 803–805, Nov. 1986.

[4] Y. Bar-Shalom, X. R. Li, and T. Kirubarajan
Estimation with Applications to Tracking and Navigation: Theory, Algorithms and Software. Wiley, Chichester, NJ, 2001.

[5] Y. Bar-Shalom, P. Willett, and X. Tian
Tracking and Data Fusion: A Handbook of Algorithms. YBS Publishing, Storrs, CT, 2011.

[6] C. Chong, S. Mori, F. Govaers, and W. Koch
"Comparison of tracklet fusion and distributed Kalman filter for track fusion,"
in *Proc. 17th Int. Conf. on Inf. Fusion (FUSION)*, Jul. 2014, pp. 1–8.

[7] C. Y. Chong and S. Mori
"Graphical models for nonlinear distributed estimation,"
in *Proc. 7th Int. Conf. Inf. Fusion*, Jul. 2004.

[8] M. Günay, U. Orguner, and M. Demirekler
"Approximate Chernoff fusion of Gaussian mixtures using sigma-points,"
in *Proc. 17th Int. Conf. on Inf. Fusion (FUSION)*, Jul. 2014, pp. 870–877.

[9] M. Günay, U. Orguner, and M. Demirekler
"Chernoff fusion of Gaussian mixtures for distributed maneuvering target tracking,"
in *Proc. 18th Int. Conf. Inf. Fusion (FUSION)*, Jul. 2015, pp. 870–877.

[10] M. B. Hurley
"An information theoretic justification for covariance intersection and its generalization,"
in *Proc. 5th Int. Conf. Inf. Fusion (FUSION)*, Jul. 2002, pp. 505–511.

[11] L. M. Kaplan, W. D. Blair, and Y. Bar-Shalom
"Simulations studies of multisensor track association and fusion methods,"
in *Proc. 2006 IEEE Aerosp. Conf.*, 2006, pp. 16.

[12] K. Lu and R. Zhou
"Sensor fusion of Gaussian mixtures for ballistic target tracking in the re-entry phase,"
Sensors, vol. 16, no. 8, Aug. 2016.

[13] R. P. S. Mahler
"Optimal/robust distributed data fusion: a unified approach,"
Proc. SPIE, vol. 4052, 2000.

[14] B. Noack, M. Reinhardt, and U. D. Hanebeck
"On nonlinear track-to-track fusion with Gaussian mixtures,"
in *Proc. 17th Int. Conf. Inf. Fusion (FUSION)*, 2014, pp. 1–8.

[15] A. C. Rencher and G. B. Schaalje
Linear Models in Statistics, 2nd ed. Wiley, Stockholm, Sweden, 2008.

Radu Visina received the Ph.D. in electrical engineering from the University of Connecticut in 2019, where he contributed to systems engineering with a focus on radar target tracking. Before pursuing graduate studies, Dr Visina designed and developed high-performance, high-precision control systems and supporting software for the sensor calibration as well as power systems industries. Dr Visina maintains expertise in the sub-fields of nonlinear estimation and feedback control, maneuvering/multiple model target tracking, nonlinear information fusion, Bayesian decision theory, and urban target tracking using non-line-of-sight radar measurement extractions. Dr Visina is currently Technical Lead Research Engineer with the Information Systems Laboratories developing real-time RF simulation tools and terrain knowledge-aided radar target tracking techniques.

Yaakov Bar-Shalom (F'84) received the B.S. and M.S. degrees from the Technion in 1963 and 1967, respectively, and the Ph.D. degree from Princeton University in 1970, all in electrical engineering. Currently he is Board of Trustees Distinguished Professor in the Electrical and Computer Engineering Department and Marianne E. Klewin Professor with the University of Connecticut. His current research interests are in estimation theory, target tracking, and data fusion. He has published more than 600 papers and book chapters. He coauthored/edited eight books, including *Tracking and Data Fusion* (YBS Publishing, 2011). In 2002, he received the J. Mignona Data Fusion Award from the DoD JDL Data Fusion Group. He is the recipient of the 2015 ISIF Award for a Lifetime of Excellence in Information Fusion. This award has been renamed in 2016 as the Yaakov Bar-Shalom Award for a Lifetime of Excellence in Information Fusion.

Peter Willett has been a faculty member in the Electrical and Computer Engineering Department at the University of Connecticut since 1986. Since 1998 he has been a Professor, and since 2003 an IEEE Fellow. He is Chief Editor for the IEEE Aerospace and Electronic Systems Magazine (2018–2020). He was Editor-in-Chief for the IEEE Signal Processing Letters, 2014–2016 and before that for the IEEE Transactions on Aerospace and Electronic Systems from 2006 to 2011. He was also the AESS Vice President for Publications from 2012 to 2014. He is a member of the IEEE Fellows Committee, Ethics Committee, and Periodicals Committee, and the IEEE Signal Processing Society's Technical Activities and Conference Boards. He is a member of the IEEE AESS Board of Governors and was Chair of IEEE Signal Processing Society's Sensor-Array and Multichannel (SAM) technical committee.

Dipak K. Dey is a Board of Trustees Distinguished Professor of Statistics with the University of Connecticut. He was the Department Head of Statistics, and later Associate Dean of Research and Physical Sciences in the College of Liberal Arts and Sciences at the University of Connecticut. He has published 10 books/edited volumes and more than 300 refereed journal articles and book chapters in various statistical and interdisciplinary journals. Currently, he is the Editor-in-Chief for *Sankhya, the Indian Journal of Statistics*. His research areas include Bayesian methodology and applications involving categorical and longitudinal data, clustering and classification, and spatio-temporal and survival data analysis.